# Paleomagnetism, magnetic anisotropy and U-Pb baddeleyite geochronology of the early Neoproterozoic Blekinge-Dalarna dolerite dykes, Sweden

Gong, Zheng

2018-10

Gong , Z , Evans , D A D , Elming , S-Å , Söderlund , U & Salminen , J M 2018 , ' Paleomagnetism, magnetic anisotropy and U-Pb baddeleyite geochronology of the early Neoproterozoic Blekinge-Dalarna dolerite dykes, Sweden ' , Precambrian Research , vol. 317 , pp. 14-32 . https://doi.org/10.1016/j.precamres.2018.08.019

http://hdl.handle.net/10138/329787
https://doi.org/10.1016/j.precamres.2018.08.019

# Paleomagnetism, magnetic anisotropy and U-Pb baddeleyite geochronology of the early Neoproterozoic Blekinge-Dalarna dolerite dykes, Sweden

Zheng Gong [a,*], David A.D. Evans [a], Sten-Åke Elming [b], Ulf Söderlund [c,d], Johanna M. Salminen [e]

[a] Department of Geology and Geophysics, Yale University, 210 Whitney Avenue, New Haven, CT 06511, USA

[b] Department of Civil, Environmental and Natural Resources Engineering, Luleå University of Technology, SE-971 87 Luleå, Sweden

[c] Department of Geology, Lund University, SE-223 62 Lund, Sweden

[d] Swedish Museum of Natural History, Laboratory of Isotope Geology, SE-104 05 Stockholm, Sweden

[e] Department of Geosciences and Geography, University of Helsinki, Helsinki 00014, Finland

* Corresponding author:
Zheng Gong (z.gong@yale.edu)

**Highlights**

- Paleomagnetism of Blekinge-Dalarna dolerite dykes demonstrates the reliability of a 951-935 Ma key pole for Baltica.
- The anomalous direction from 947 Ma Nornäs dyke is attributed to a partial remagnetization.
- Baltica and Laurentia drifted from high to low latitude between 970-960 Ma and 950-935 Ma, and returned back to high latitude by 920-870 Ma.
- The Blekinge-Dalarna dolerite dykes are unlikely a giant circumferential swarm generated by a mantle plume.

**Abstract**

Paleogeographic proximity of Baltica and Laurentia in the supercontinent Rodinia has been widely accepted. However, robust paleomagnetic poles are still scarce, hampering quantitative tests of proposed relative positions of the two cratons. A recent paleomagnetic study of the early Neoproterozoic Blekinge-Dalarna dolerite (BDD) dykes in Sweden provided a 946-935 Ma key pole for Baltica, but earlier studies on other BDD dykes discerned large variances in paleomagnetic directions that appeared to indicate more complicated motion of Baltica, or alternatively, unusual geodynamo behavior in early Neoproterozoic time. We present combined paleomagnetic, rock magnetic, magnetic fabric and geochronological studies on BDD dykes in the Dalarna region, southern Sweden. Positive baked-contact and paleosecular variation tests support the reliability of the 951-935 Ma key pole (Paleolatitude = -2.6°N, Paleolongitude = 239.6°E, $A_{95}$ = 5.8°, N = 12 dykes); and the ancient magnetic field was likely a stable geocentric axial dipole at that time, based on a positive reversal test. Detailed analysis of the 947 Ma Nornäs dyke, one of the dykes previously showing anomalous directions, suggests a partial viscous remagnetization. Therefore, the observed large variances in nearly coeval BDD dykes are suspected to result from present-day overprints that were not adequately removed in earlier studies. In addition, we obtained a 971 Ma virtual geomagnetic pole (Paleolatitude = -27.0°N, Paleolongitude = 230.4°E, $A_{95}$ = 14.9°, N = 4 dykes) for Baltica. Comparing similar-aged poles from Laurentia, we suggest that Baltica and Laurentia drifted together from high to low latitude between 970-960 Ma and 950-935 Ma, and returned back to high latitude by 920-870 Ma. In this scenario, the apparent polar wander paths of Baltica and Laurentia may be more complicated than the previously proposed, solitary Sveconorwegian and Grenville loops. The new U-Pb baddeleyite ages do not support BDD dykes as a giant circumferential swarm generated by a mantle plume, and the prolonged timespan of dyke intrusion is likely associated with the plate boundary forces as causing gravitational extension at the waning stage of the Sveconorwegian orogeny.

**Keywords**

Blekinge-Dalarna dolerite (BDD) dykes; Sveconorwegian loop; Baltica; paleomagnetism; magnetic anisotropy; U-Pb baddeleyite geochronology

## 1. Introduction

Although the existence of the Proterozoic supercontinent Rodinia has long been suggested, its configuration is still highly debated, and new studies continue to paint different pictures regarding the shape of Rodinia (e.g., Slagstad et al., 2013; Wen et al., 2017; Wen et al., 2018). Nonetheless, the juxtaposition of Laurentia and Baltica in Rodinia is widely adopted in various reconstruction models (e.g., Dalziel, 1997; Pisarevsky et al., 2003; Cawood and Pisarevsky, 2006; Li et al., 2008; Evans, 2009), in order to account for geological similarities between the two cratons. As the only quantitative method to constrain the paleolatitude and the orientation of pre-Pangea continents, paleomagnetism plays an important role in testing current reconstruction models of Laurentia and Baltica. The apparent polar wander (APW) paths of Laurentia and Baltica, including the Grenville and Sveconorwegian loops, respectively, show a broad agreement during post-1.0-Ga Rodinia assembly (Li et al., 2008), supporting the paleogeographic proximity of the two cratons. However, most paleomagnetic poles on the Grenville and Sveconorwegian loops derive from high-grade metamorphic rocks, making the determination of the age of remanence acquisition difficult (Brown and McEnroe, 2012; Brown and McEnroe, 2015). Compilation of paleomagnetic poles with ages between 1.3 Ga and 0.9 Ga (Veikkolainen et al., 2017) shows that even though numerous poles have been generated for Baltica and Laurentia, high-quality poles with quality criteria $Q_{Voo}$ value larger than 4 are scarce (Fig.1a), and most poles have no field tests to constrain the age of remanence (Fig. 1b). As a result, large uncertainties remain regarding the shapes and younging directions of the Grenville and Sveconorwegian loops (Hyodo and Dunlop, 1993; Elming et al., 1993; Weil et al., 2006; Elming et al., 2014).

Mafic intrusions are promising targets for yielding high-quality poles since they are usually enriched in magnetite grains. Also, baddeleyite grains in mafic intrusions can be directly dated by U-Pb method with high precision (Söderlund et al., 2005). A recent study of the Blekinge-Dalarna dolerite (BDD) dykes in southern Sweden generated a 946-935 Ma low-latitude pole that has been proposed as a key pole for Baltica (Elming et al., 2014). However, earlier studies of BDD dykes show large variances in paleomagnetic directions (Patchett and Bylund, 1977; Bylund, 1985; Bylund and Elming, 1992) that might indicate unusual cratonic motions or complicated geomagnetic behavior. Here we present detailed paleomagnetic, rock magnetic and magnetic fabric studies on a number of BDD dykes in the Dalarna region, southern Sweden, in order to better understand the paleogeography of Baltica in early Neoproterozoic time. We also present new U-Pb baddeleyite ages that shed light on the tectonic origin of BDD dykes.

**2. Geologic background, previous work and sampling**

Following the Svecofennian orogeny (2.0-1.75 Ga), Baltica grew outward as a result of accretionary tectonics manifested by the 1.81-1.76 Ga Transscandinavian Igneous Belt (TIB; Bogdanova et al., 2015). Afterwards, there was a protracted interval of mafic magmatism peaked at 1.6 Ga, 1.57 Ga, 1.47-1.44 Ga, 1.27-1.26 Ga, 1.22 Ga, and 0.98-0.95 Ga, respectively (Söderlund et al., 2005; Brander and Söderlund, 2007). The 1.47-1.44 Ga magmatism, referred to as the Danopolonian event (Bogdanova et al., 2001), is largely coeval with dynamic high-grade metamorphism in southwestern Sweden, and is suggested to be related to convergent active margin processes called the Hallandian event (Christoffel et al., 1994; Söderlund et al., 2002; Möller et al., 2007; Brander and Söderlund, 2007). After the Hallandian event, the 1.1-0.9 Ga Sveconorwegian orogeny (e.g., Bingen et al., 2008) extensively reworked the basement rocks west of the Protogine Zone (PZ) and the Sveconorwegian Frontal Deformation Zone (SFDZ) in southwest Scandinavia (Fig. 2; Wahlgren et al., 1994). Later, Caledonian allochthons were thrust onto the northwest margin of Baltica at 0.6-0.4 Ga (Fig. 2; Gaál and Gorbatschev, 1987; Bingen and Solli, 2009).

Partly coincident with the Sveconorwegian orogeny, the early Neoproterozoic BDD dykes intruded the TIB and Svecofennian rocks east of the PZ and SFDZ, over an extent of 750 km (Fig. 2). One prominent feature of BDD dykes is their arcuate shape, trending NE-SW in the Blekinge region, and deflected ~60° to NW-SE in the Dalarna region (Fig. 2). The ages of BDD dykes are well established by U-Pb baddeleyite geochronology and $^{40}Ar/^{39}Ar$ whole-rock dating, ranging from 978 Ma to 939 Ma (Söderlund et al., 2005; Elming et al., 2014). The origin of BDD dykes is debated. Different models have been proposed, including fracturing due to late Sveconorwegian uplift (Patchett and Bylund, 1977), gravitational collapse at the final stage of the Sveconorwegian orogeny (Pisarevsky and Bylund, 2006), and the giant circumferential system of a mantle plume (Buchan and Ernst, 2016). Petrological studies show that BDD dykes are fine- to medium-grained with slight alteration, and the major minerals consist of plagioclase, olivine, clinopyroxene, orthopyroxene, biotite, ilmenite, and titanomagnetite (Johansson and Johansson, 1990; Solyom et al., 1992).

Previous paleomagnetic work focused on the southern and central part of BDD dykes (e.g., Patchett and Bylund, 1977; Bylund, 1985; Bylund and Elming, 1992), while the northern part is relatively less studied. Recently, Elming et al. (2014) proposed a low-latitude pole for Baltica at 946-935 Ma, combining the results of several BDD dykes in the Norrköping and Falun areas with the 935 Ma Göteborg-Slussen dykes in southwestern Sweden (Fig. 2; Pisarevsky and Bylund, 2006). The reliability of this low-latitude pole is supported by a positive baked-contact test and the appearance of antipodal directions. However, large variances still remain in the paleomagnetic results of BDD dykes, complicating the application of the low-latitude pole to paleogeographic reconstruction of Baltica. For example, the 947 Ma Nornäs dyke yields a high-latitude pole (Piper and Smith, 1980; Bylund, 1985), which apparently contradicts with the result of Elming et al. (2014). It is also difficult to explain their difference by plate tectonics because they are very similar in age and would imply extremely rapid continental motions. Alternative interpretations have been suggested, such as late-stage selective remagnetization, true polar wander, a non-dipole geomagnetic field or the non-averaged paleosecular variation (Pesonen and Klein, 2013). However, none of these has been fully examined. Notably, the result of the Nornäs dyke was obtained more than three decades ago when modern laboratory treatment and data analysis of paleomagnetism had not been fully developed. Hence, it is necessary to restudy the Nornäs dyke with more detailed and sophisticated techniques.

Since more than 90% of the bedrock in the Dalarna region is covered by glacial deposits, aeromagnetic data (Ripa et al., 2012) and data from geological mapping of the Swedish Geological Survey (Ripa, personal communication) were used to help delineate dykes in the field. For detailed mapping of the outcrops, a portable magnetic susceptibility meter was used to determine the extension of the dykes and contacts to host rocks. A number of NW-SE trending dykes in the Dalarna region were sampled using a portable gasoline-powered rock drill (Fig. 3). Host rocks (ca. 1.46 Ga Öje basalt and ca. 1.46 Ga Dala sandstone) were collected in two sites for baked-contact tests, the former where a clear intrusive contact was observed, and the latter where the concealed contact could be triangulated to within about a meter of the baked host-rock samples. Core samples were oriented with a Brunton compass, and sun-compass readings were also taken in order to correct any small-scale magnetic anomaly in the outcrop. Block samples were collected from the central parts of dykes for U-Pb baddeleyite geochronology.

## 3. Methods

### 3.1 U-Pb baddeleyite geochronology

All samples were crushed, and baddeleyite grains were separated using the Wilfley table technique following Söderlund and Johansson (2002) at Lund University in Sweden. The extracted baddeleyite grains are dark to moderately brown. Grains from all samples are fresh without any trace of alteration. About 1-5 grains per fraction were combined and transferred to clean Teflon capsules. Grains were washed in numerous steps using 3 M $HNO_3$, including one step on a hotplate (~30 minutes). One drop of the $^{205}$Pb-$^{233-236}$U tracer solution and 10 drops of HF-$HNO_3$ (10:1) were added to each capsule. Baddeleyite grains were completely dissolved after 3 days in an oven under high pressure at a temperature of ~190°C. The samples were evaporated on a hotplate and then dissolved in 10 drops of 6.2 M HCl. One drop of 0.25 M $H_3PO_4$ was added to each capsule before it dried down. U and Pb were loaded on an outgassed Re filament together with a small amount of silica gel.

Thermal Ionization Mass Spectrometry (TIMS) was performed at the Laboratory of Isotope Geology at the Swedish Museum of Natural History in Stockholm, Sweden, using a Thermo Finnigan Triton TIMS system. An ETP SEM detector equipped with a RPQ filter was used to measure the Pb and U isotope intensities in dynamic (peak-switching) mode. Pb-isotopes were measured at a filament temperature in the 1200-1230°C range, while U-isotopes were measured in dynamic mode on the SEM with filament temperatures exceeding 1300°C. Data reduction was performed using the Excel add-in "Isoplot" of Ludwig (2003); decay constants for $^{238}U$ and $^{235}U$ follow those of Jaffey et al. (1971). All errors in age and isotopic ratios are quoted at 2σ. Initial Pb isotope compositions were corrected according to the global common Pb evolution model of Stacey and Kramers (1975). U-Pb data are presented in Table 1 and the fractions are plotted in the concordia diagrams in Fig. 4.

3.2 Magnetic measurements

Magnetic measurements were conducted in the Paleomagnetic Laboratory and Archaeomagnetism Laboratory at Yale University, USA. In order to understand the pattern of dyke propagation and to discern the possible alteration or deformation of dykes (Hrouda, 1982; Rochette et al., 1992), anisotropy of magnetic susceptibility (AMS) was measured for each dyke using an AGICO Kappabridge KLY-4S susceptibility meter. AMS data were analyzed in Anisoft42 software. To characterize magnetic mineralogy, representative samples were subjected to thermomagnetic susceptibility analysis. Temperature ranges from 25°C to 700°C and is controlled by a CS3 high temperature furnace apparatus. Bulk magnetic susceptibility was measured during heating and cooling in an argon gas environment in order to subdue magnetic phase transition. Magnetic grain size was inferred by the Day plot (Day et al., 1977) constructed by magnetic parameters, which are determined by hysteresis loop measurement using a MicroMag 2900 alternating gradient magnetometer (AGM). After the measurement of natural remanent magnetization (NRM), samples were cooled to liquid nitrogen temperature (~77 K) in a magnetic shielded container to demagnetize the remanence carried by multidomain grains (Muxworthy and McClelland, 2000). Thermal demagnetization was conducted in an ASC Scientific TD-48 thermal demagnetizer with stepwise heating up to 580°C in 15-20 steps in a nitrogen gas environment. Sister samples from each dyke were demagnetized using alternating field (AF) in a Molspin tumbler demagnetizer. After each thermal or AF demagnetization step, remanence was measured by a 2G Enterprises cryogenic DC-SQuID magnetometer with automatic sample-changing device (Kirschvink et al., 2008). Paleomagnetic vectors were calculated using principal component analysis (Kirschvink, 1980) and the great circle method (McFadden and McElhinny, 1988), and were plotted using vector-endpoint diagrams

(Zijderveld, 1967) in PaleoMag X software (Jones, 2002). Paleogeographic reconstruction was carried out using GPlates software (Boyden et al., 2011).

## 4. Results

### 4.1 U-Pb baddeleyite geochronology

We report U-Pb baddeleyite TIMS ages of three NW-SE trending BDD dykes from the Dalarna region. Data are summarized in Table 1, and concordia diagrams are shown in Fig. 4. Three baddeleyite fractions of dyke G16S12, which is intrusive into the Öje basalt (G16S11), are concordant at 951 ± 5 Ma (2σ, mean square weighted deviates [MSWD] = 1.4). This age is calculated as the weighted mean of $^{207}Pb/^{206}Pb$ dates for these fractions. Three fractions of dyke G16S22 were analyzed, of which two are concordant within uncertainty whereas one analysis is slightly discordant. The weighted mean of $^{207}Pb/^{206}Pb$ dates is 971 ± 7 Ma (2σ, MSWD = 0.61). Three fractions of dyke G16S37, which is probably the southern extension of the Nornäs dyke, cluster at and just below the concordia curve. The weighted mean is 947 ± 4 Ma (2σ, MSWD = 2.8). These age estimates are interpreted as dating the crystallization of the rocks.

Before this study, a total of 11 ages of BDD dykes/sills were published, with nine U-Pb baddeleyite ages (Söderlund et al., 2004a; Söderlund et al., 2005) and two $^{40}Ar/^{39}Ar$ whole-rock ages (Elming et al., 2014). We provide an additional three U-Pb baddeleyite ages. Collectively, they demonstrate a ~40 million-year range of BDD intrusions with probably three magmatic pulses, extending from 978 Ma to 939 Ma (Fig. 5).

### 4.2 Rock magnetism

AMS data show that the degree of anisotropy ($P_j$) of BDD dykes is typically below 6%, which is a common value for primary fabric of igneous rocks (Hrouda, 1982). Low $P_j$ values indicate that these rocks have not experienced significant deformation, hence, have a reasonable chance of retaining primary magnetization. The majority of dykes exhibit oblate fabrics with $K_{max}$ and $K_{int}$ axes dispersed in the NW-SE oriented, vertical or sub-vertical plane (Fig. 6e). Some dykes show prolate fabrics with $K_{max}$ axis pointing to the NW-SE direction (Fig. 6a). The orientation of magnetic anisotropy ellipsoid genuinely reflects the trends (NW-SE) of these dykes (Knight and Walker, 1988), which is also supported by field observations and the aeromagnetic anomaly map (Fig. 3; Ripa et al., 2012). AMS of Öje basalt is expected to have a horizontal oblate fabric; the $K_{min}$ axis shows a transition from steep to shallow directions (Fig. 6c). Samples with shallow $K_{min}$ axes are close to the contact and the chilled margin of dyke G16S12. It is suspected that some secondary magnetic minerals might grow along the basalt contact zone due to the migration of reducing fluids, and cause anomalously shallow $K_{min}$ axes. But the remanences of the secondary magnetic minerals are adequately removed by thermal demagnetization and have no effect on primary paleomagnetic signals (see discussion below). AMS of the Dala sandstone (G16S24) shows a typical depositional fabric (oblate and horizontal), with $K_{min}$ axis perpendicular to the bedding plane and $K_{max}$ and $K_{int}$ axes distributed parallel to the bedding plane (Fig. 6h).

Thermomagnetic susceptibility analysis of BDD dykes shows that heating and cooling curves are generally reversible (Fig. 7). During heating, the magnetic susceptibility decreases substantially between 580°C and 600°C, which provides clear evidence for the presence of magnetite. Minor drops in magnetic susceptibility are also noticed between 600°C and 700°C, indicating small amounts of hematite or maghemite. Exceptions are Öje basalt (G16S11) and dyke G16S12, which yields a distinct susceptibility hump and a large decline between 300°C and 400°C on the heating curve (Fig. 7c-d). This temperature range coincides with the Curie temperature of magnetic sulfides (pyrrhotite or greigite). During heating, the magnetic sulfides were broken down to form new magnetite, as suggested by the sharply increased susceptibility at 580°C on the cooling curve. The magnetic sulfides are likely the reason for shallow $K_{min}$ axis observed in the AMS data of Öje basalt (G16S11). Dala sandstone (G16S24) has a low magnetic susceptibility and shows a gradual decrease in susceptibility between 600°C and 700°C (Fig. 7g), suggesting the major magnetic phase is hematite or titano-hematite.

The coercivity of remanence of BDD dykes determined by hysteresis loop measurement is typically less than 30 mT, which is a normal value for magnetite. Only dyke G16S12 gives slightly higher coercivity (~80 mT), showing the contribution from magnetic sulfides (Fig. 8b). The typical grain size of magnetic phases in BDD dykes falls in pseudo-single domain (PSD) region on the Day plot. According to Dunlop (2002)’s theoretical estimates, the magnetic grains are mixtures of single domain (SD) and multidomain (MD) minerals with varying SD content ranging from 20% to 60% (Fig. 8c).

### 4.3 Paleomagnetism

Paleomagnetic results show that during heating, most samples exhibit a significant decline of remanence at ~580°C, close to the unblocking temperature for pure magnetite (Fig. 9). Samples that were subjected to liquid nitrogen bath show a large decrease of remanence, indicating that the viscous remanence carried by MD grains has been effectively removed (Fig. 9). Some samples show a gradual loss of remanence at lower temperatures, which could be either due to the demagnetization of larger size grains or magnetic sulfides. Most samples yield a clear decay-to-origin component between 500°C and 580°C, which is defined as the characteristic remanent magnetization (ChRM). Only samples from sites G16S17 and G16S18 (two sites were collected from the same dyke) were analyzed by the combination of principal component analysis and great circle method, owing to the overlapping unblocking temperatures of different-sized grains.

Usable paleomagnetic directions of BDD dykes fall into two statistically different groups (Fig. 10a), one with shallower inclinations (Group A) and another with steeper inclinations (Group B). Importantly, the dating results also show that the two groups are different in age. Group A is about 951 ± 5 Ma, ~20 million years younger than Group B (971 ± 7 Ma). Both groups show two polarities. Following Precambrian paleomagnetism database PALEOMAGIA's nomenclature (Veikkolainen et al., 2017), we assign reverse polarity to sites with southeasterly declinations (Groups Ar, Br) and normal polarity to sites with northwesterly declinations (Groups An, Bn; Table 2). Paleomagnetic directions of Group A are resemble those of the Y1, Y2 and Falun dykes obtained in Elming et al. (2014). A positive baked-contact test supports the primary origin of the NW-up direction (Group An; Elming et al., 2014), In addition, we have two positive baked-contact tests for the SE-down direction (Group Ar). The baked areas of the Öje basalt (G16S11) and the Dala sandstone (G16S24), which were intruded by dykes G16S12 and G16S23 respectively, show similar remanence to BDD dykes, but are very different from their primary (unbaked) directions (Piper and Smith, 1980; Fig. 10a). We performed a reversal test on

Group A, together with Y1, Y2 and Falun dykes from Elming et al. (2014) and the Tuve, Small, Hjuvik and Slussen dykes from Pisarevsky and Bylund (2006); the test is demonstrated to be positive with classification C ($\gamma/\gamma_c$ = 8.7°/13.9°; McFadden and McElhinny, 1990). On the basis of the similar ages and paleomagnetic results of Pisarevsky and Bylund (2006), Elming et al. (2014), and our data, we obtained a new mean 951-935 Ma paleomagnetic pole: Paleolatitude = -2.6°N, Paleolongitude = 239.6°E, $A_{95}$ = 5.8° (N = 12 dykes; Table 2). There is no baked-contact test for the four dykes in Group B, but their demagnetization patterns, such as the square-shouldered thermal decay curve with the unblocking temperature closed to 580°C, suggest that their ChRMs are probably primary (Fig. 9). The number of dykes in Group B is insufficient for the reversal test, but quasi-antipodal directions have been observed, also supporting the notion that dykes in Group B carry primary remanence. We calculated a 971 Ma virtual geomagnetic pole (VGP) from Group B, which is Paleolatitude = -27.0°N, Paleolongitude = 230.4°E, $A_{95}$ = 14.9° (N = 4 dykes; Table 2).

Paleomagnetic results of the Nornäs dyke (G16S05 and G16S06; 946.8 ± 1.2 Ma) show that the natural remanent magnetization (NRM) direction is very close to the steep ChRM yielded from previous work (Piper and Smith, 1980; Bylund, 1985). The steep ChRM is also very close to present-day field (PDF) direction (Fig. 10b). However, as temperature or AF intensity increases, the inclination gradually decreases (Fig. 11). It is noteworthy that the direction of remanences of some samples are able to migrate towards the upper hemisphere at ~570°C or ~30 mT. The remanence becomes unstable when approaching the unblocking temperature or coercivity of magnetite, so it is hard to isolate a decay-to-origin component. However, the directions move towards the NW-up BDD-reference direction (Group An; Fig. 10). The pattern of vector-endpoint diagrams clearly shows a partial remagnetization. Based on the aeromagnetic anomaly map and geochronology, it is likely that sites G16S16 and G16S37 (947 ± 4 Ma) are from a southeastward extension of the Nornäs dyke, and they also give identical paleomagnetic results and similar ages. Therefore, we interpret that the Nornäs dyke consists of some PSD grains that carry a PDF overprint, difficult to be adequately removed due to the strong overlap of unblocking temperature or coercivity with SD magnetite grains. Since a clear decay-to-origin component cannot be isolated from sites G16S05, G16S06, G16S16 and G16S37, we tried to use great circle method for paleomagnetic analyses. Combining all great circles from these four sites of the Nornäs dyke, we obtained a mean direction of Declination = 307.9°, Inclination = -35.3°, $\alpha_{95}$ = 2.9°, which we named it as "Nornäs new", the direction of which is very close to the NW-up BDD-reference direction (Group An; Fig. 10; Table 2). The Nornäs new direction is likely the primary remanence of the Nornäs dyke. However, without any sample bearing a clear decay-to-origin component, we prefer to exclude this Nornäs new mean direction from the paleomagnetic statistics of this study. The steep ChRM direction of previous work was calculated from the minimum scatter in magnetic directions after demagnetization in AF intensities of 10-20 mT (Piper and Smith, 1980; Bylund, 1985; Table 2), which is too low to remove the PDF overprint. Another dyke, G16S14, yields similar demagnetization pattern as the Nornäs dyke and is also likely affected by partial remagnetization in the PDF direction.

## 5. Discussion

### 5.1 Origin of BDD dykes – A giant circumferential swarm?

Arcuate-shaped swarms have been increasingly reported in different geological settings with various intrusion ages (Denyszyn et al., 2009; Mäkitie et al., 2014; Buchan and Ernst, 2018). However, the physical mechanism explaining the unusual geometry is still under debate. Interestingly, the coronae on Venus are also characterized by similar ring-shaped surface expressions and are thought to be associated with tectono-magmatic processes (Squyres et al., 1992). Are the arcuate-shaped swarms on Earth and Venusian coronae intrinsically related in terms of their origin?

Venusian coronae have two components: a radiating system and a circumferential system, both of which are presumably underlain by dykes (Ernst et al., 2003). In order to explain their distinctive tectonic and topographic features, Stofan and Head (1990) suggested a mantle plume origin for coronae. The radiating system is argued to be related to the upwelling of hot magma, causing surface uplift and dyke intrusion, while the circumferential system is due to gravitational collapse as the mantle upwelling ceases. If this mechanism is true, it is expected that the radiating system would predate the circumferential system.

Ernst and Buchan (1998) first proposed that the arcuate-shaped swarms on the Earth could be analogous to Venusian coronae. They defined any arcuate-shaped swarm as a giant circumferential swarm if it has a primary circular or elliptical geometry with an arc of > 45° and a diameter > 60 km (Buchan and Ernst, 2016). Based on these criteria, BDD dykes would be classified as a giant circumferential swarm, accounting for their 750-km long, ~60° arcuate geometry. The primary curved geometry is supported by tectonic coherence of southern Sweden since Neoproterozoic time, and also the demonstrably high-quality BDD paleomagnetic data, which discern no structural rotation following emplacement. Therefore, the critical test of this hypothesis hinges on another two aspects. Is there a corresponding radiating system? And if so, is the radiating system older than BDD dykes, as required by Stofan and Head (1990)'s model?

The available ages of BDD dykes/sills suggest prolonged intrusions (Fig. 5). Given the distribution of these ages, there seems to be 3 possible pulses of BDD intrusions, first pulse from 980 Ma to 965 Ma; second from 955 Ma to 945 Ma; third from 942 Ma to 935 Ma (Fig. 5), although definitive conclusion still needs more geochronological studies. Any radiating-system candidate should be older or at least very close to the first pulse of BDD intrusions. The Göteborg-Slussen dykes in southwestern Sweden were proposed as the radiating system linked to the purported mantle plume, because their trends are sub-orthogonal to those of the BDD dykes (Fig. 2; Buchan and Ernst, 2016). However, the Tuve dyke, which belongs to the Göteborg-Slussen dyke suite, is dated to be 935 ± 3 Ma by the U-Pb baddeleyite method (Hellström et al., 2004), which approaches equivalency to the youngest members of BDD dykes but is tens of millions of years younger than the majority of BDD dykes. Another candidate for the radiating system might be the Hunnedalen dykes in western Norway (Fig. 2), trending NE-SW, sub-orthogonal to BDD dykes. But the Hunnedalen dykes are ~100 million years younger than BDD dykes (Walderhaug et al., 1999), excluding their possibility of being the radiating component. In general, geochronological data do not support Buchan and Ernst (2016)'s mantle plume model. The prolonged intrusion interval of BDD dykes is more likely connected with the plate boundary forces causing gravitational extension in the Baltic foreland during protracted waning stages of the Sveconorwegian orogeny. Variable orientation of the regional stress field might be the cause for the primary arcuate geometry (Wahlgren et al., 1994).

## 5.2 Implications for paleogeography of Baltica

Large variances have been observed in the paleomagnetic results of BDD dykes (Fig. 10b; Table 2), which have been interpreted differently in previous studies (e.g., Pesonen and Klein, 2013). Here, we summarize available paleomagnetic and geochronological data of BDD dykes in the literature (Fig. 5; Table 2), in an attempt to examine each proposed model, and then discuss their implications. First, if we assume that all BDD results are reliable without any remagnetization/contamination, the variance in BDD dyke remanences would be substantial (Table 2), for instance, the very steep inclinations of 947 Ma Nornäs dyke and 954 Ma Karlshamn dyke, and the very shallow inclinations of 946 Ma Fäjö dyke and 948 Ma Bräkne-Hoby dyke (Fig. 10b). This variance, occurring within a fairly short time interval (< 10 Ma), if interpreted as plate motion, would require unrealistically fast drift rates of Baltica, contradicting geologically younger plate tectonic speeds. Even true polar wander, which might occur as fast as ~6° per Myr (Rose and Buffett, 2017), is insufficient to reconcile the variances in BDD remanences. Another possibility might be a non-GAD field, but even then, the entire BDD dataset would be difficult to explain unless departures from GAD were extreme. For example, Pesonen et al. (2012) show that with 11% octupole field (relative to a dominant GAD field), the inclination shallowing effect will approach a maximum ~10° at mid-paleolatitudes. However, the inclination differences among BDD remanences are mostly larger than 10°, and some even reach 70-80° (Table 2). Only if the transient ancient magnetic field was totally dominated by octupole component (Tauxe, 2005) or by an ephemeral equatorial dipole field (Abrajevitch and Van der Voo, 2010) can the large inclination differences be explained.

After the experience gained from careful demagnetization procedures in our study, we are suspicious that the large variances of remanence in the entire BDD dataset likely result from selective remagnetization. The 947 Ma Nornäs dyke, after being subjected to detailed demagnetization, shows that the remanence gradually moves away from the previously determined ChRM and towards the NW-up BDD-reference direction (Figs. 10 and 11). In fact, based on the great circle analyses, the primary remanence of the Nornäs dyke should be the same as that of Group An, and the low-temperature or low-AF remanence component of Nornäs dyke is NNW and steep down, very close to the PDF direction. Hence, it is very likely that the Nornäs dyke was affected by partial remagnetization and component mixing due to overlapping coercivity and/or unblocking temperature spectra. That concept impels us to doubt the robustness of other anomalous directions, especially the 954 Ma Karlshamn dyke, for which the published ChRM direction is very close to the PDF direction (Fig. 10b). Also, as the remanences of 946 Ma Lösen-Fäjö and 948 Ma Bräkne-Hoby dykes are half-way between the PDF direction and the NW-up BDD-reference direction (Group An), they could possibly carry substantial PDF overprints as well. Besides, the previously published directions of the Nornäs, Lösen-Fäjö, Karlshamn and Bräkne-Hoby dykes were calculated using the minimum scatter of data at 10 mT, 20 mT, 30 mT or 40 mT (Patchett and Bylund, 1977; Piper and Smith, 1980; Bylund, 1985; Table 2). AF demagnetization below 30 mT is generally too low to be pertinent to Precambrian paleomagnetic remanence preservation. If two components have strongly overlapping demagnetization spectra, higher AF intensities do not necessarily guarantee a successful removal of a partial overprint. With more sophisticated laboratory equipment and more accurate analytical methods (principal component analysis, great circle method etc.) now available, we suggest a re-study of these dykes before using their directions for geophysical interpretations.

Because we suspect the reliability of some results of BDD dykes in previous studies, either due to the inadequate demagnetization (e.g., low AF field) or outdated analytical methods (e.g., least scatter method for averaging paleomagnetic directions), for subsequent discussion we only focus on the results that we can be assured to lack an overprint/contamination. This would yield 12 dykes in Group A (6 dykes in Group An and 6 dykes in Group Ar; Table 2) and 4 dykes in Group B (1 dyke in Group Bn and 3 dykes in Group Br; Table 2). We admit that by this treatment the paleomagnetic dataset of BDD dykes is reduced, but we can test for averaging out the paleosecular variation (PSV) by calculating the angular dispersion (S) for each of the two poles we obtained from Groups A and B, respectively, following the approximation equation:

$$S = \frac{81^\circ}{\sqrt{k}}$$

where k is the best estimate of precision parameter (Butler, 1992).

The calculated S values are plotted against the 1.5-0.5 Ga model G curve fitted by Veikkolainen and Pesonen (2014). It is noted that the 951-935 Ma pole obtained from Group A matches the model G curve very well (Fig. 12; Table 3), which means that even though we used a smaller dataset, the number of dykes seems sufficient to average out the PSV. In contrast, the 971 Ma pole obtained from Group B falls below the model G curve (Fig. 12; Table 3). Since there are only 4 dykes in Group B, this pole is considered merely as a VGP, and more dykes in this group are needed to provide a paleomagnetic pole in future studies. Further geochronology on Group B dykes would also be useful to assess whether they are restricted to a narrow age range.

The early Neoproterozoic apparent polar wander (APW) path of Baltica, known as the Sveconorwegian loop, is under debate in terms of its shape and form. Previously, the Sveconorwegian loop (as shown in the South Pacific) was generally assumed to exhibit counterclockwise motion (Fig. 13a; Elming et al., 1993). However, some have suggested that the southernmost part of the Sveconorwegian loop represents a post-900 Ma delayed remanence acquisition during slow exhumation of the deep-seated igneous rocks (Walderhaug et al., 1999; Brown and McEnroe, 2004). Pisarevsky and Bylund (2006) speculated that the delayed acquisition is probably caused by low-temperature chemical alteration. Elming et al. (2014) proposed a clockwise motion of the south-Pacific polarity representation of the Sveconorwegian loop, incorporating the 945 Ma equatorial pole and assuming that the southernmost part of the loop is post-900 Ma (Fig. 13a). Similarly, the early Neoproterozoic APW path of Laurentia (also viewed in the south-Pacific polarity representation) is also interpreted as either clockwise (Hyodo and Dunlop, 1993) or counterclockwise (Weil et al., 2006). Regardless of uncertainties in the APW paths of two cratons, geological evidence supports a proximity of Baltica and Laurentia during the Neoproterozoic time (Cawood and Pisarevsky, 2006).

Our results from the BDD dykes support the equatorial pole for Baltica at 951-935 Ma, similar to the result of Elming et al. (2014). In addition, we obtained a 971 Ma VGP for Baltica, suggesting a high-paleolatitude position. Brown and McEnroe (2012) studied paleomagnetism of the igneous and metamorphic rocks in the Adirondack Highlands of Laurentia. Performing careful rock-magnetic and petrological studies, they generated several poles with modeled cooling ages of 990-960 Ma. We also performed the PSV test of the 970 Ma and 960 Ma poles from Brown and McEnroe (2012), which suggests that the PSV has been averaged out from these two poles (Fig. 12; Table 3). Cratonic reconstruction using these poles and our new 971 Ma VGP permits a close position between Baltica and Laurentia at 970-960 Ma. The reconstructed positions of two cratons allow the Sveconorwegian and Grenville orogenies be a continuous belt, which has been suggested in many other studies (e.g., Li et al., 2008; although see Gower et al., 2008, for cautionary details). The Sveconorwegian and Grenville loops seem to have some oscillatory components (Fig. 13), which could be attributed to plate motions or true polar wander (Evans, 2009). In this scenario, the paleogeographic evolution of the two cratons is characterized by high- to low-latitude drift between 970-960 Ma and 950-935 Ma, and a return from low to high latitude by 920-870 Ma (Fig. 14). Notably, all three pole groups include at least one result that appears to average paleosecular variation adequately (Fig. 12). The implied drifting speeds of ~100-150 km/Ma, which is fast but is a reasonable rate for either plate tectonics or true polar wander. Deconvolving those two processes will require more detailed paleomagnetic work from Baltica, Laurentia, and other cratons with suitably complete early Neoproterozoic geological records.

## 6. Conclusions

We present a detailed paleomagnetic, rock magnetic and anisotropy of magnetic susceptibility, and geochronological study of the Blekinge-Dalarna dolerite dykes, which leads to following conclusions:

(1) Positive baked-contact, reversal and PSV tests support the reliability of the equatorial paleomagnetic pole for Baltica at 951-935 Ma (Paleolatitude = -2.6°N, Paleolongitude = 239.6°E, $A_{95}$ = 5.8°, N = 12 dykes), which can be used as a key pole to constrain the paleogeography of Baltica.

(2) The anomalous paleomagnetic direction obtained from the 947 Ma Nornäs dyke is probably due to a PDF overprint that was not adequately removed by low alternating-field

demagnetization levels in previous studies, instead of originating from true polar wander, or abnormal geomagnetic field behaviors. PDF component contamination is suspected in other anomalously-directed BDD dykes.

(3) A well-dated 971 Ma VGP (Paleolatitude = -27.0°N, Paleolongitude = 230.4°E, $A_{95}$ = 14.9°) from four BDD dykes, in concert with same-age poles from Laurentia, suggests a high-latitude position for Baltica in proto-Rodinia. Paleogeographic reconstruction demonstrates that Baltica and Laurentia drifted together towards low latitude between 970-960 Ma and 950-935 Ma, and moved back to high latitude by 920-870 Ma. In this scenario, the apparent polar wander path would be more complicated than either the Sveconorwegian and Grenville loops considered in isolation.

(4) Based on published ages of BDD dykes and adjacent dykes sub-orthogonal to it, it seems that the requirement of a single mantle plume model is not satisfied. The BDD dykes more likely result from plate boundary forces associated with the Sveconorwegian orogeny. The arcuate geometry could be associated with a spatially varying regional stress distribution.

**Acknowledgements**

We would like to thank Anna Sartell at Lund University for preparing baddeleyite grains for U-Pb dating, and Stephen Victor for helping with hysteresis loop measurement in Yale Archaeomagnetism Laboratory. Thanks are also due to Magnus Ripa at the Geological Survey of Sweden for the geological data and information of outcrops, and to Torkhild Rasmussen at Luleå University of Technology for help in creating maps of outcrops. Two anonymous reviewers are gratefully acknowledged for constructive reviews that improved the quality of the manuscript.

**References**

Abrajevitch, A., & Van der Voo, R. (2010). Incompatible Ediacaran paleomagnetic directions suggest an equatorial geomagnetic dipole hypothesis. Earth and Planetary Science Letters, 293(1-2), 164-170.

Bingen, B., Nordgulen, Ø., Viola, G. (2008). A four-phase model for the Sveconorwegian orogeny, SW Scandinavia. Norsk Geologisk Tidsskrift, 88, 43-72.

Bingen, B., & Solli, A. (2009). Geochronology of magmatism in the Caledonian and Sveconorwegian belts of Baltica: synopsis for detrital zircon provenance studies. Norwegian Journal of Geology, 89, 267-290.

Bogdanova, S.V., Page, L.M., Skridlaite, G., & Taran, L.N. (2001). Proterozoic tectonothermal history in the western part of the East European Craton: $^{40}$Ar/$^{39}$Ar geochronological constraints. Tectonophysics, 339, 39-66.

Bogdanova, S., Gorbatschev, R., Skridlaite, G., Soesoo, A., Taran, L., & Kurlovich, D. (2015). Trans-Baltic Palaeoproterozoic correlations towards the reconstruction of supercontinent Columbia/Nuna. Precambrian Research, 259, 5-33.

Boyden, J. A., Müller, R. D., Gurnis, M., Torsvik, T. H., Clark, J. A., Turner, M., Ivey-Law, H., Watson, R. J., & Cannon, J. S. (2011). Next-generation plate-tectonic reconstructions using GPlates. Geoinformatics, 9, 5-114.

Brander, L., & Söderlund, U. (2009). Mesoproterozoic (1.47–1.44 Ga) orogenic magmatism in Fennoscandia; Baddeleyite U–Pb dating of a suite of massif-type anorthosite in S. Sweden. International Journal of Earth Science (Geologische Rundschau), 98, 499-516.

Brown, L. L., & McEnroe, S. A. (2004). Palaeomagnetism of the Egersund-Ogna anorthosite, Rogaland, Norway, and the position of Fennoscandia in the Late Proterozoic. Geophysical Journal International, 158(2), 479-488.

Brown, L. L., & McEnroe, S. A. (2012). Paleomagnetism and magnetic mineralogy of Grenville metamorphic and igneous rocks, Adirondack Highlands, USA. Precambrian Research, 212, 57-74.

Brown, L. L., & McEnroe, S. A. (2015). 916 Ma pole for southwestern Baltica: Palaeomagnetism of the Bjerkreim-Sokndal layered intrusion, Rogaland igneous complex, southern Norway. Geophysical Journal International, 203(1), 567-587.

Buchan, K. L., & Ernst, R. E. (2016). Giant circumferential dyke swarms on Earth: Possible analogues of coronae on Venus and similar features on Mars. Acta Geologica Sinica (English Edition), 90(sup.1): 186-187.

Buchan, K. L., & Ernst, R. E. (2018). A giant circumferential dyke swarm associated with the High

Arctic Large Igneous Province (HALIP). Gondwana Research, 58, 39-57.

Butler, R. F. (1992). Paleomagnetism: magnetic domains to geologic terranes (Vol. 319). Boston: Blackwell Scientific Publications.Bylund, G. (1985). Palaeomagnetism of middle Proterozoic basic intrusives in central Sweden and the Fennoscandian apparent polar wander path. Precambrian Research, 28(3-4), 283-310.

Bylund, G., & Elming, S. Å. (1992). The Dala dolerites, central Sweden, and their palaeomagnetic signature. GFF, 114(1), 143-153.

Cawood, P. A., & Pisarevsky, S. A. (2006). Was Baltica right-way-up or upside-down in the Neoproterozoic? Journal of the Geological Society, 163(5), 753-759.

Christoffel, C., Connelly, J.N., Åhäll, K.-I. (1999) Timing and characterization of recurrent pre-Sveconorwegian metamorphism and deformation in the Varberg-Halmstad region of SW Sweden. Precambrian Research, 98, 173-195.

Dalziel, I. W. (1997). Neoproterozoic-Paleozoic geography and tectonics: Review, hypothesis, environmental speculation. Geological Society of America Bulletin, 109(1), 16-42.

Day, R., Fuller, M., & Schmidt, V. A. (1977). Hysteresis properties of titanomagnetites: Grain-size and compositional dependence. Physics of the Earth and planetary interiors, 13(4), 260-267.

Denyszyn, S. W., Davis, D. W., & Halls, H. C. (2009). Paleomagnetism and U-Pb geochronology of the Clarence Head dykes, Arctic Canada: Orthogonal emplacement of mafic dykes in a large igneous province. Canadian Journal of Earth Sciences, 46(3), 155-167.

Dunlop, D. J. (2002). Theory and application of the Day plot (Mrs/Ms versus Hcr/Hc) 1. Theoretical curves and tests using titanomagnetite data. Journal of Geophysical Research: Solid Earth, 107(B3).

Elming, S. Å., Pesonen, L. J., Leino, M. A. H., Khramov, A. N., Mikhailova, N. P., Krasnova, A. F., Merlanen, S., Bylund, G., & Terho, M. (1993). The drift of the Fennoscandian and Ukrainian shields during the Precambrian: A palaeomagnetic analysis. Tectonophysics, 223(3-4), 177-198.

Elming, S. Å., Pisarevsky, S. A., Layer, P., & Bylund, G. (2014). A palaeomagnetic and $^{40}Ar/^{39}Ar$ study of mafic dykes in southern Sweden: A new Early Neoproterozoic key-pole for the

Baltic Shield and implications for Sveconorwegian and Grenville loops. Precambrian Research, 244, 192-206.

Ernst, R.E., Buchan, K.L. (1998). Arcuate dyke swarms associated with mantle plumes on Earth: Implications for Venusian coronae. Lunar and Planetary Science Conference #29, Houston, Texas, Abstract #1021.

Ernst, R. E., Desnoyers, D. W., Head, J. W., & Grosfils, E. B. (2003). Graben-fissure systems in Guinevere Planitia and Beta Regio (264°-312°E, 24°-60°N), Venus, and implications for regional stratigraphy and mantle plumes. Icarus, 164(2), 282-316.

Evans, D. A. D. (2009). The palaeomagnetically viable, long-lived and all-inclusive Rodinia supercontinent reconstruction. Geological Society, London, Special Publications, 327(1), 371-404.

Gaál, G., & Gorbatschev, R. (1987). An outline of the Precambrian evolution of the Baltic Shield. Precambrian Research, 35, 15-52.

Gower, C.F., Kamo, S., & Krogh, T.E. (2008). Indentor tectonism in the eastern Grenville Province. Precambrian Research, 167, 201-212.

Hellström, F. A., Johansson, Å., & Larson, S. Å. (2004). Age and emplacement of late Sveconorwegian monzogabbroic dykes, SW Sweden. Precambrian Research, 128(1), 39-55.

Hrouda, F. (1982). Magnetic anisotropy of rocks and its application in geology and geophysics. Surveys in Geophysics, 5(1), 37-82.

Hyodo, H., & Dunlop, D. J. (1993). Effect of anisotropy on the paleomagnetic contact test for a Grenville dike. Journal of Geophysical Research: Solid Earth, 98(B5), 7997-8017.

Jaffey, A. H., Flynn, K. F., Glendenin, L. E., Bentley, W. T., & Essling, A. M. (1971). Precision measurement of half-lives and specific activities of $^{235}U$ and $^{238}U$. Physical Review C, 4(5), 1889-1906.

Johansson, L., & Johansson, Å. (1990). Isotope geochemistry and age relationships of mafic intrusions along the Protogine Zone, southern Sweden. Precambrian Research, 48(4), 395-414.

Jones, C. H. (2002). User-driven integrated software lives: “Paleomag” paleomagnetics analysis on the Macintosh. Computers & Geosciences, 28(10), 1145-1151.

Kirschvink, J. L. (1980). The least-squares line and plane and the analysis of palaeomagnetic data. Geophysical Journal International, 62(3), 699-718.

Kirschvink, J. L., Kopp, R. E., Raub, T. D., Baumgartner, C. T., & Holt, J. W. (2008). Rapid, precise, and high sensitivity acquisition of paleomagnetic and rock magnetic data: Development of a low noise automatic sample changing system for superconducting rock magnetometers. Geochemistry, Geophysics, Geosystems, 9(5).

Knight, M. D., & Walker, G. P. (1988). Magma flow directions in dikes of the Koolau Complex, Oahu, determined from magnetic fabric studies. Journal of Geophysical Research: Solid Earth, 93(B5), 4301-4319.

Tauxe, L. (2005). Inclination flattening and the geocentric axial dipole hypothesis. Earth and Planetary Science Letters, 233(3-4), 247-261.

Mäkitie, H., Data, G., Isabirye, E., Mänttäri, I., Huhma, H., Klausen, M. B., Pakkanen, L., & Virransalo, P. (2014). Petrology, geochronology and emplacement model of the giant 1.37 Ga arcuate Lake Victoria Dyke Swarm on the margin of a large igneous province in eastern Africa. Journal of African Earth Sciences, 97, 273-296.

Meert, J. G., & Torsvik, T. H. (2003). The making and unmaking of a supercontinent: Rodinia revisited. Tectonophysics, 375(1-4), 261-288.

Mertanen, S., Pesonen, L. J., & Huhma, H. (1996). Palaeomagnetism and Sm-Nd ages of the Neoproterozoic diabase dykes in Laanila and Kautokeino, northern Fennoscandia. Geological Society, London, Special Publications, 112(1), 331-358.

McFadden, P. L., & McElhinny, M. W. (1988). The combined analysis of remagnetization circles and direct observations in palaeomagnetism. Earth and Planetary Science Letters, 87(1-2), 161-172.

McFadden, P. L., & McElhinny, M. W. (1990). Classification of the reversal test in palaeomagnetism. Geophysical Journal International, 103(3), 725-729.

Möller, C., Andersson, A., Lundqvist, I., Hellström, F. (2007) Linking deformation, migmatite formation and zircon U-Pb geochronology in polymetamorphic orthogneisses, Sveconorwegian Province, Sweden. Journal of Metamorphic Geology, 25, 727-750.

Muxworthy, A. R., & McClelland, E. (2000). Review of the low-temperature magnetic properties of magnetite from a rock magnetic perspective. Geophysical Journal International, 140(1), 101-114.

Patchett, P. J., & Bylund, G. (1977). Age of Grenville belt magnetisation: Rb-Sr and palaeomagnetic evidence from Swedish dolerites. Earth and Planetary Science Letters, 35(1), 92-104.

Pesonen, L. J., & Klein, R. (2013). Paleomagnetism of some Proterozoic sediments and diabases, South Sweden. Abstract in XXVI Geofysiikan Päivät 2013, 93-96.

Pesonen, L. J., Mertanen, S., & Veikkolainen, T. (2012). Paleo-Mesoproterozoic supercontinents – A paleomagnetic view. Geophysica, 48(1-2), 5-47.

Piper, J. D., & Smith, R. L. (1980). Palaeomagnetism of the Jotnian lavas and sediments and post-Jotnian dolerites of central Scandinavia. GFF, 102(2), 67-81.

Pisarevsky, S. A., Wingate, M. T., Powell, C. M., Johnson, S., & Evans, D. A. (2003). Models of Rodinia assembly and fragmentation. Geological Society, London, Special Publications, 206(1), 35-55.

Pisarevsky, S. A., & Bylund, G. (2006). Palaeomagnetism of 935 Ma mafic dykes in southern Sweden and implications for the Sveconorwegian Loop. Geophysical Journal International, 166(3), 1095-1104.

Poorter, R. P. E. (1975). Palaeomagnetism of Precambrian rocks from southeast Norway and south Sweden. Physics of the Earth and Planetary Interiors, 10(1), 74-87.

Li, Z. X., Bogdanova, S. V., Collins, A. S., Davidson, A., De Waele, B., Ernst, R. E., Fitzsimons, I. C. W., Fuck, R. A., Gladkochub, D. P., Jacobs, J. & Karlstrom, K. E. (2008). Assembly, configuration, and break-up history of Rodinia: A synthesis. Precambrian Research, 160(1), 179-210.

Ludwig, K. R. (2003). User's manual for isoplot 3.00, a geochronlogical toolkit for microsoft excel. Berkeley Geochronl. Cent. Spec. Publ., 4, 25-32.

Lundmark, A. M., & Lamminen, J. (2016). The provenance and setting of the Mesoproterozoic Dala Sandstone, western Sweden, and paleogeographic implications for southwestern Fennoscandia. Precambrian Research, 275, 197-208.

Ripa, M., Mellqvist, C., Ahl, M., Andersson, D., Bastani, M., Delin, H., Kübler, L., Nyston, P., Persson, L. & Thelander, T. (2012). Bedrock map Western part of the county Dalarna, scale 1:250 000. Sveriges Geologiska Undersökning K 382.

Rochette, P., Jackson, M., & Aubourg, C. (1992). Rock magnetism and the interpretation of anisotropy of magnetic susceptibility. Reviews of Geophysics, 30(3), 209-226.

Rose, I., & Buffett, B. (2017). Scaling rates of true polar wander in convecting planets and moons. Physics of the Earth and Planetary Interiors, 273, 1-10.

Slagstad, T., Roberts, N. M., Marker, M., Røhr, T. S., & Schiellerup, H. (2013). A non-collisional, accretionary Sveconorwegian orogen. Terra Nova, 25(1), 30-37.

Söderlund, U., & Johansson, L. (2002). A simple way to extract baddeleyite ($ZrO_2$). Geochemistry, Geophysics, Geosystems, 3(2).

Söderlund, U., Möller, C., Andersson, J., Johansson, L., & Whitehouse, M. (2002) Zircon geochronology in polymetamorphic gneisses in the Sveconorwegian orogen, SW Sweden: ion microprobe evidence for 1.46-1.42 and 0.98-0.96 Ga reworking. Precambrian Research, 113, 193-225.

Söderlund, U., Patchett, P. J., Vervoort, J. D., & Isachsen, C. E. (2004a). The $^{176}$Lu decay constant determined by Lu-Hf and U-Pb isotope systematics of Precambrian mafic intrusions. Earth and Planetary Science Letters, 219(3), 311-324.

Söderlund, P., Söderlund, U., Möller, C., Gorbatschev, R., & Rodhe, A. (2004b). Petrology and ion microprobe U-Pb chronology applied to a metabasic intrusion in southern Sweden: A study on zircon formation during metamorphism and deformation. Tectonics, 23(5).

Söderlund, U., Isachsen, C. E., Bylund, G., Heaman, L. M., Patchett, P. J., Vervoort, J. D., & Andersson, U. B. (2005). U-Pb baddeleyite ages and Hf, Nd isotope chemistry constraining repeated mafic magmatism in the Fennoscandian Shield from 1.6 to 0.9 Ga. Contributions to Mineralogy and Petrology, 150(2), 174-194.

Söderlund, U., Elming, S. Å., Ernst, R. E., & Schissel, D. (2006). The central Scandinavian dolerite Group-Protracted hotspot activity or back-arc magmatism? Constraints from U-Pb baddeleyite geochronology and Hf isotopic data. Precambrian Research, 150(3), 136-152.

Solyom, Z., Lindqvist, J. E., & Johansson, I. (1992). The geochemistry, genesis, and geotectonic setting of Proterozoic mafic dyke swarms in southern and central Sweden. GFF, 114(1), 47-65.

Squyres, S. W., Janes, D. M., Baer, G., Bindschadler, D. L., Schubert, G., Sharpton, V. L., & Stofan, E. R. (1992). The morphology and evolution of coronae on Venus. Journal of Geophysical Research: Planets, 97(E8), 13611-13634.

Stacey, J. T., & Kramers, J. D. (1975). Approximation of terrestrial lead isotope evolution by a two-stage model. Earth and Planetary Science Letters, 26(2), 207-221.

Stearn, J. E. F., & Piper, J. D. A. (1984). Palaeomagnetism of the Sveconorwegian mobile belt of the Fennoscandian Shield. Precambrian Research, 23(3-4), 201-246.

Stofan, E. R., & Head, J. W. (1990). Coronae of Mnemosyne Regio: Morphology and origin. Icarus, 83(1), 216-243.

Van der Voo, R. (1990). The reliability of paleomagnetic data. Tectonophysics, 184(1), 1-9.

Veikkolainen, T., & Pesonen, L. J. (2014). Palaeosecular variation, field reversals and the stability of the geodynamo in the Precambrian. Geophysical Journal International, 199(3), 1515-1526.

Veikkolainen, T. H., Biggin, A. J., Pesonen, L. J., Evans, D. A., & Jarboe, N. A. (2017). Advancing Precambrian palaeomagnetism with the PALEOMAGIA and PINT ($_{QPI}$) databases. Scientific data, 4, 170068.

Wahlgren, C. H., Cruden, A. R., & Stephens, M. B. (1994). Kinematics of a major fan-like structure in the eastern part of the Sveconorwegian orogen, Baltic Shield, south-central Sweden. Precambrian Research, 70(1-2), 67-91.

Walderhaug, H. J., Torsvik, T. H., Eide, E. A., Sundvoll, B., & Bingen, B. (1999). Geochronology and palaeomagnetism of the Hunnedalen dykes, SW Norway: Implications for the Sveconorwegian apparent polar wander loop. Earth and Planetary Science Letters, 169(1), 71-83.

Walderhaug, H. J., Torsvik, T. H., & Halvorsen, E. (2007). The Egersund dykes (SW Norway): A robust early Ediacaran (Vendian) palaeomagnetic pole from Baltica. Geophysical Journal International, 168(3), 935-948.

Weil, A. B., Geissman, J. W., & Ashby, J. M. (2006). A new paleomagnetic pole for the Neoproterozoic Uinta Mountain Supergroup, central Rocky Mountain states, USA. Precambrian Research, 147(3), 234-259.

Wen, B., Evans, D. A., & Li, Y. X. (2017). Neoproterozoic paleogeography of the Tarim Block: An extended or alternative “missing-link” model for Rodinia? Earth and Planetary Science Letters, 458, 92-106.

Wen, B., Evans, D. A., Wang, C., Li, Y. X., & Jing, X. (2018). A positive test for the Greater Tarim Block at the heart of Rodinia: Mega-dextral suturing of supercontinent assembly. Geology, 46(8): 687-690.

Zijderveld, J.D.A. (1967). AC demagnetization of rocks: analysis of results. Methods paleomagnetism 3, 254.

**Figure captions**

Fig.1 Compilation of paleomagnetic poles from Baltica and Laurentia within the 1.3-0.9 Ga interval (Veikkolainen et al., 2017). (a) Sum of quality criteria $Q_{(6)}$ (Van der Voo, 1990), excluding the seventh criterion as in the Precambrian paleomagnetism database PALEOMAGIA. (b) Individual quality criteria (Van der Voo, 1990). N = number of paleomagnetic poles.

Fig. 2 Geologic map of southern Sweden. GÄZ = Göta Älv Zone, MZ = Mylonite Zone, PZ = Protogine Zone, SFDZ = Sveconorwegian Frontal Deformation Zone. Inset map shows the major tectonic divisions of southern Sweden (modified from Söderlund et al., 2004b). GS = Göteborg-Slussen dykes, Hu = Hunnedalen dykes, RIC = Rogaland Igneous Complex. Small boxes show the locations of Y1, Y2 (Y), and Falun (F) dykes in Elming et al. (2014); and Lösen-Fäjö (L), Bräkne-Hoby (B), Karlshamn (K), and Härsjön (H) dykes in Patchett and Bylund (1977); and Nornäs dyke (N) in this study.

Fig. 3 Geologic map of the western Dalarna region (modified from Lundmark and Lamminen, 2016). Proterozoic dyke locations are based on Ripa et al. (2012). Sites yield interpretable paleomagnetic results (white) and sites give paleomagentically unstable directions/partial remagnetization (black) are differentiated by colors.

Fig. 4 U-Pb concordia diagrams of dated BDD dykes.

Fig. 5 Summary of ages from 980-930 Ma BDD-related intrusions in southern Sweden. Age references are listed in Table 2. Shaded areas show age ranges of possible pulses of BDD intrusions.

Fig. 6 Representative stereonet projections of the anisotropy of magnetic susceptibility (AMS) data. Squares, triangles and circles show the principal axes of AMS ellipsoids. Grey arrows indicate the trends of dykes inferred from aeromagnetic anomalies (Ripa et al., 2012). Red arrow represents the evolution of AMS ellipsoid of Öje basalt.

Fig. 7 Results of thermomagnetic susceptibility analysis. Heating and cooling curves are represented by red and blue colors, respectively.

Fig. 8 Hysteresis ratios of BDD dykes displayed in the Day plot (Day et al., 1977). The dashed line shows the SD/MD theoretical mixing curve (Dunlop, 2002). Inset plots are representative hysteresis loops after the correction of paramagnetic slope.

Fig. 9 Representative thermal demagnetization results of BDD dykes. Vector-endpoint diagrams are shown (Zijderveld, 1967), with equal-area stereonet plots and remanence intensity ($J/J_0$) plots. ChRMs are plotted with blue and red arrows representing declinations and inclinations, respectively.

Fig. 10 (a) Equal-area stereonet projection summarizing the ChRMs of BDD dykes with corresponding 95% confidence cones. Unbaked paleomagnetic direction of Öje basalt and Dala sandstone is suggested by the purple diamond. Present-day field direction of sampling area is indicated by the black square. Closed and open circles show the downwards and upwards paleomagnetic inclinations. PDF = present-day field. (b) Equal-area stereonet projection of anomalous BDD dyke directions. Red stars indicate the BDD reference directions.

Fig. 11 Typical thermal and alternating-field demagnetization behaviors of the Nornäs dyke. Vector-endpoint diagrams (Zijderveld, 1967), equal-area stereonet plots and remanence intensity ($J/J_0$) plots are shown. Red solid/dashed lines indicate the trending of remanent directions in lower/upper hemisphere.

Fig. 12 Paleosecular variation (PSV) test. The thick black line is the 1.5-0.5 Ga model G curve from Veikkolainen and Pesonen (2014). The gray area is the corresponding error limits ($2\sigma$). Numbers are paleomagnetic poles used in the paleogeographic reconstruction, which are listed in Table 3.

Fig. 13 (a) Sveconorwegian loop for Baltica. Counterclockwise motion is from Elming et al. (1993) and clockwise motion is from Elming et al. (2014). (b) Grenville loop for Laurentia. Counterclockwise motion is from Weil et al. (1998) and clockwise motion is from Hyodo and Dunlop (1993). (c) Coeval 1000-850 Ma paleomagnetic poles from Baltica and Laurentia in present North America reference frame. White arrows indicate the younging directions of apparent polar wander paths. Blue dash lines indicate new loop proposed by this study. Red poles are from Baltica and green poles are from Laurentia. Poles' numbers are listed in Table 3.

Fig. 14 Paleogeographic reconstructions of Baltica and Laurentia. (a) 970-960 Ma (Euler pole of Laurentia to absolute reference: 22.4°N, 100.6°E, 127.6°; Euler pole of Baltica to Laurentia: 75.8°N, 95.7°E, -59.2°); (b) 950-935 Ma (Euler pole of Laurentia to absolute reference: -37.9°N, -65.5°E, -99.8°; Euler pole of Baltica to Laurentia: 75.8°N, 95.7°E, -59.2°); (c) 920-870 Ma (Euler pole of Laurentia to absolute reference: -15.6°N, -93.5°E, -125.9°; Euler pole of Baltica to Laurentia: 75.8°N, 95.7°E, -59.2°). Paleomagnetic poles used for reconstruction are listed and numbered in Table 3. Dark and light gray poles are from Baltica and Laurentia, respectively.

**Table captions**

Table 1 Results of U-Pb baddeleyite geochronology.

Table 2 Summary of paleomagnetic results of BDD dykes.

Table 3 Paleomagnetic poles constrain the early Neoproterozoic paleogeographic reconstruction of Baltica and Laurentia.

# Figure 1

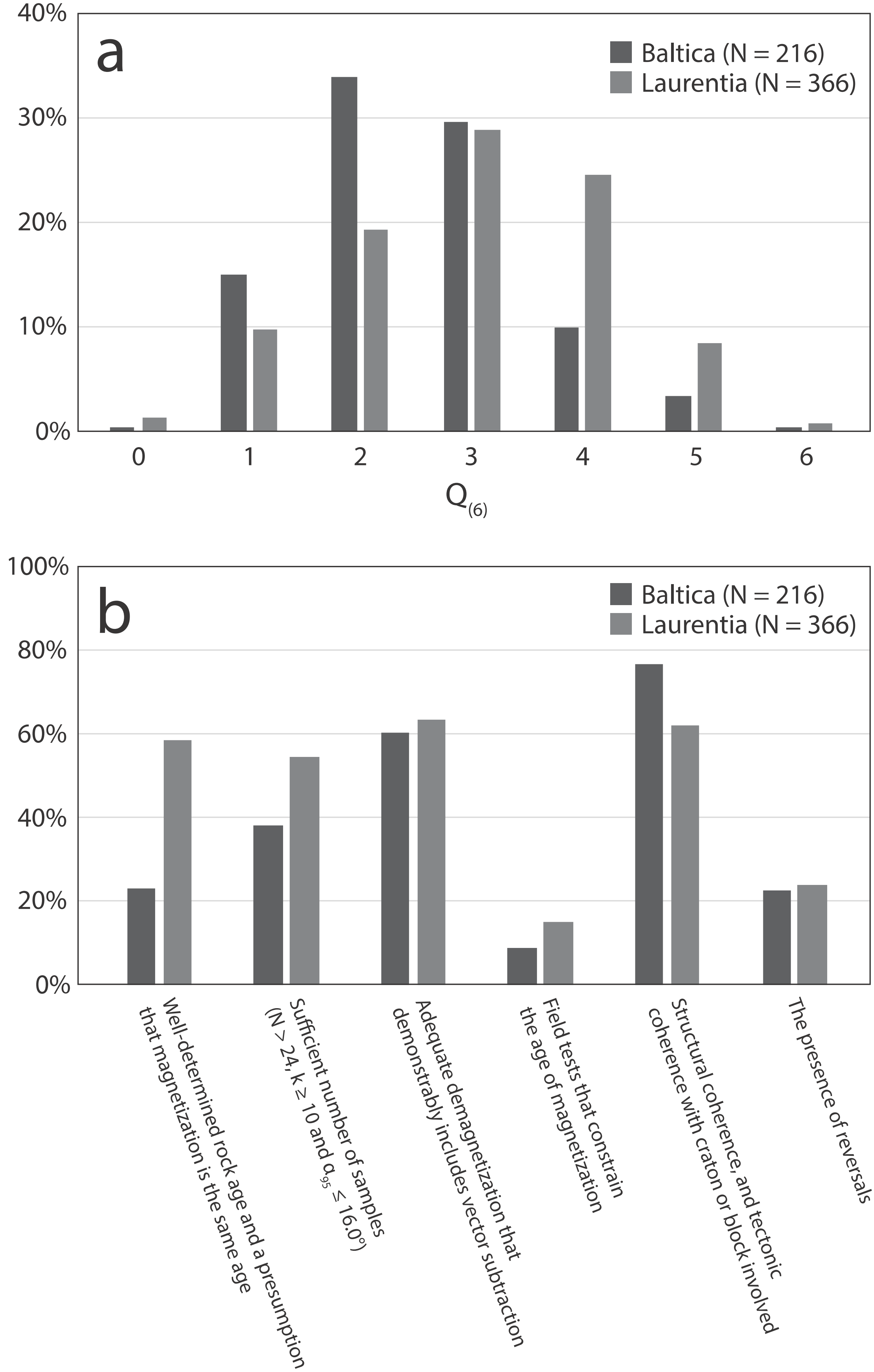

a
Baltica (N = 216)
Laurentia (N = 366)
40%
30%
20%
10%
0%
0
1
2
3
4
5
6
Q(6)
b
Baltica (N = 216)
Laurentia (N = 366)
100%
80%
60%
40%
20%
0%
Well-determined rock age and a presumption that magnetization is the same age
Sufficient number of samples (N > 24, k ≥ 10 and α95 ≤ 16.0°)
Adequate demagnetization that demonstrably includes vector subtraction
Field tests that constrain the age of magnetization
Structural coherence, and tectonic coherence with craton or block involved
The presence of reversals

# Figure 2

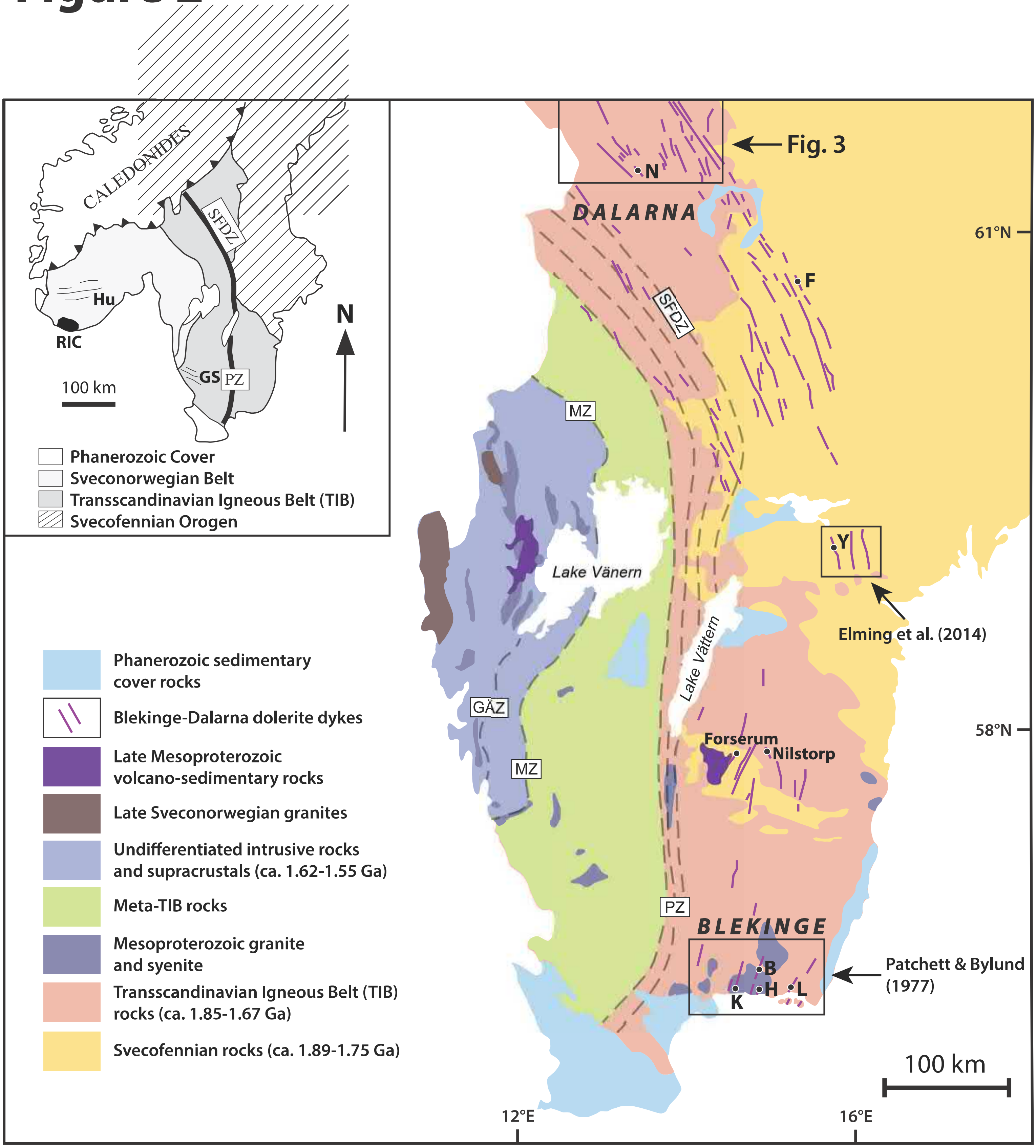

CALEDONIDES
SFDZ
Hu
RIC
GS
PZ
100 km
N
Phanerozoic Cover
Sveconorwegian Belt
Transscandinavian Igneous Belt (TIB)
Svecofennian Orogen
Fig. 3
N
DALARNA
61°N
F
SFDZ
MZ
Lake Vänern
Y
Elming et al. (2014)
Lake Vättern
GÄZ
MZ
58°N
Forserum
Nilstorp
PZ
BLEKINGE
B
H
L
K
Patchett & Bylund (1977)
100 km
12°E
16°E
Phanerozoic sedimentary cover rocks
Blekinge-Dalarna dolerite dykes
Late Mesoproterozoic volcano-sedimentary rocks
Late Sveconorwegian granites
Undifferentiated intrusive rocks and supracrustals (ca. 1.62-1.55 Ga)
Meta-TIB rocks
Mesoproterozoic granite and syenite
Transscandinavian Igneous Belt (TIB) rocks (ca. 1.85-1.67 Ga)
Svecofennian rocks (ca. 1.89-1.75 Ga)

# Figure 3

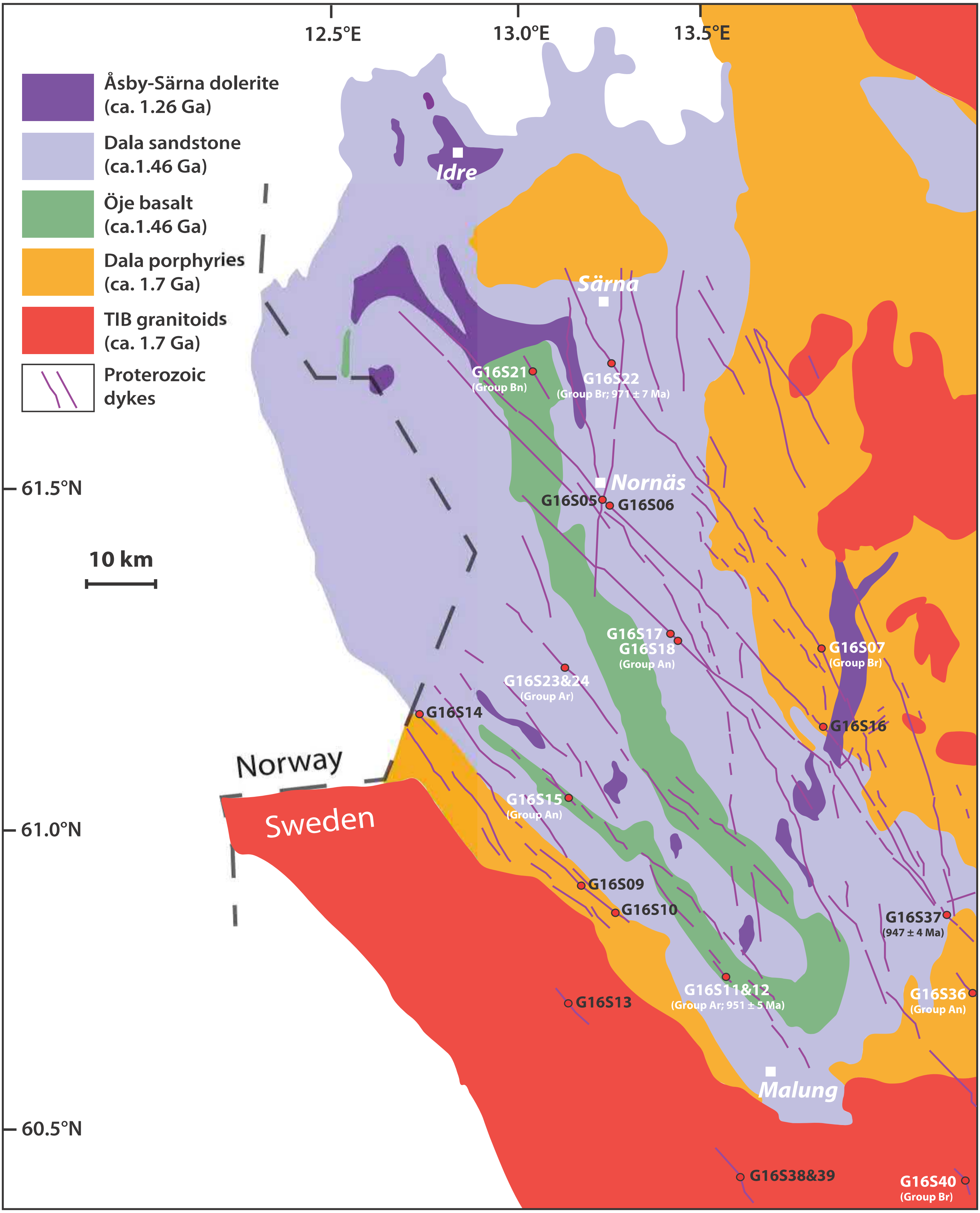

12.5°E
13.0°E
13.5°E
61.5°N
61.0°N
60.5°N
Åsby-Särna dolerite (ca. 1.26 Ga)
Dala sandstone (ca.1.46 Ga)
Öje basalt (ca.1.46 Ga)
Dala porphyries (ca. 1.7 Ga)
TIB granitoids (ca. 1.7 Ga)
Proterozoic dykes
10 km
Idre
Särna
Nornäs
Malung
Norway
Sweden
G16S21 (Group Bn)
G16S22 (Group Br; 971 ± 7 Ma)
G16S05
G16S06
G16S17
G16S18 (Group An)
G16S07 (Group Br)
G16S23&24 (Group Ar)
G16S14
G16S16
G16S15 (Group An)
G16S09
G16S10
G16S37 (947 ± 4 Ma)
G16S11&12 (Group Ar; 951 ± 5 Ma)
G16S13
G16S36 (Group An)
G16S38&39
G16S40 (Group Br)

**Figure 4**

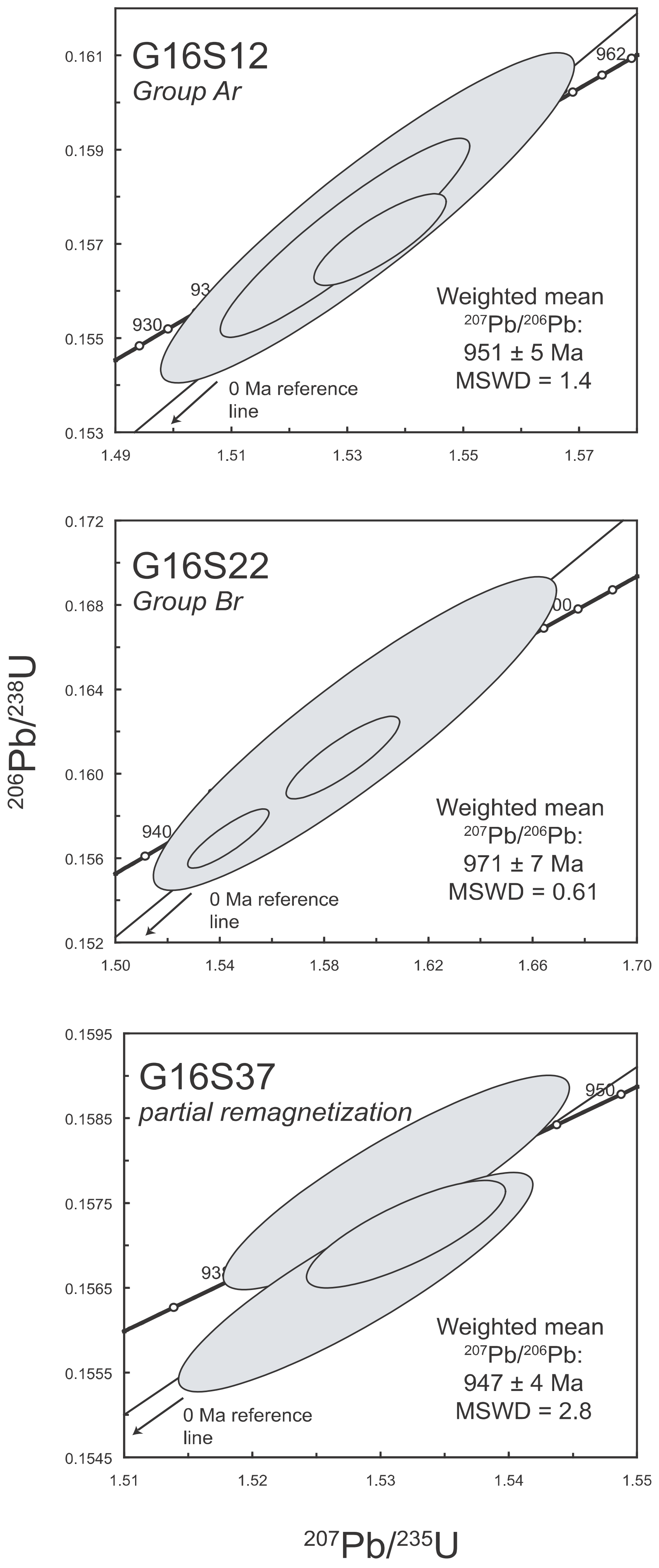
G16S12
Group Ar
962
930
93
Weighted mean
207Pb/206Pb:
951 ± 5 Ma
MSWD = 1.4
0 Ma reference line
G16S22
Group Br
940
Weighted mean
207Pb/206Pb:
971 ± 7 Ma
MSWD = 0.61
0 Ma reference line
G16S37
partial remagnetization
950
Weighted mean
207Pb/206Pb:
947 ± 4 Ma
MSWD = 2.8
0 Ma reference line
206Pb/238U
207Pb/235U

# Figure 5

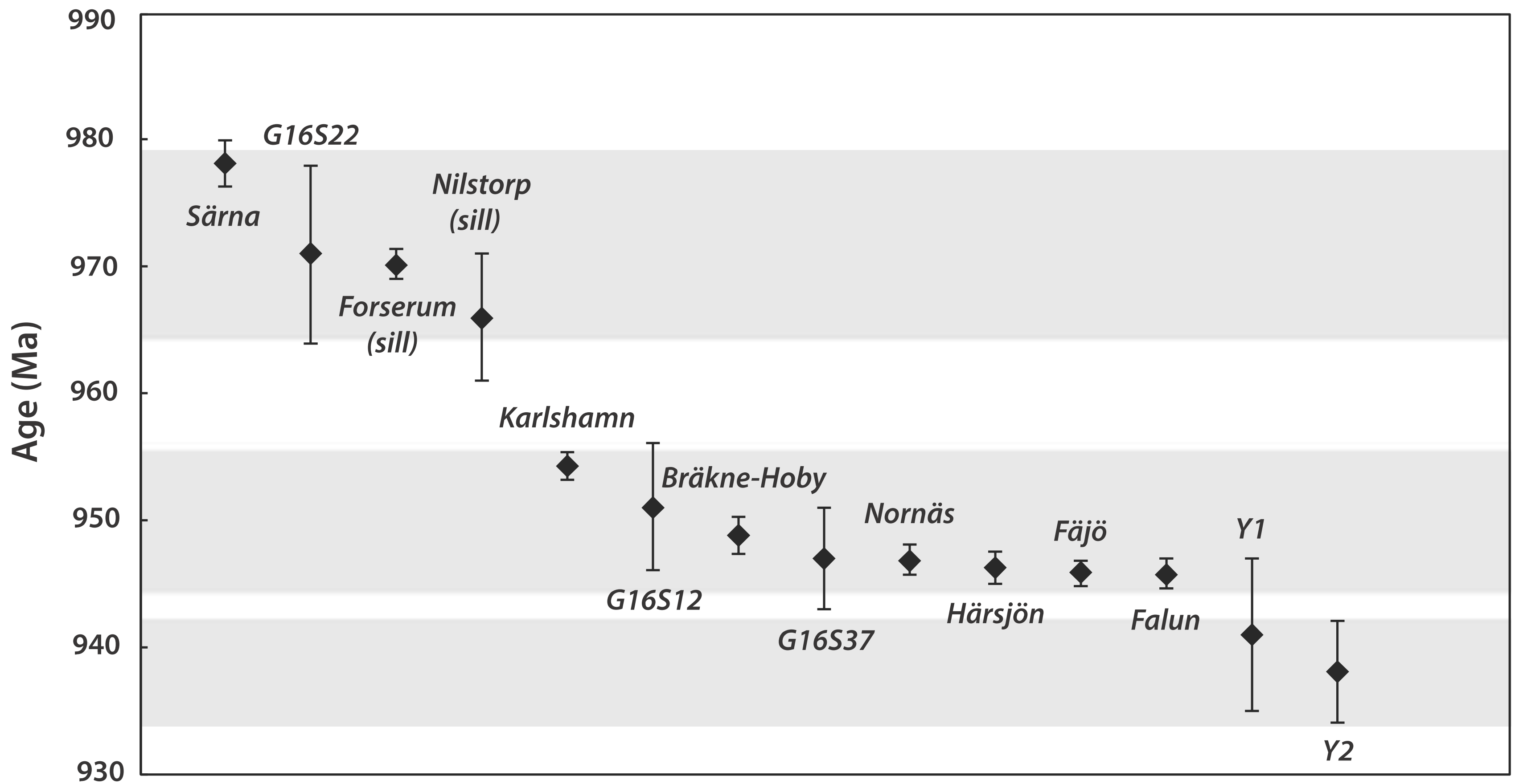
Age (Ma)
990
980
970
960
950
940
930
Särna
G16S22
Forserum
(sill)
Nilstorp
(sill)
Karlshamn
G16S12
Bräkne-Hoby
G16S37
Nornäs
Härsjön
Fäjö
Falun
Y1
Y2

# Figure 6

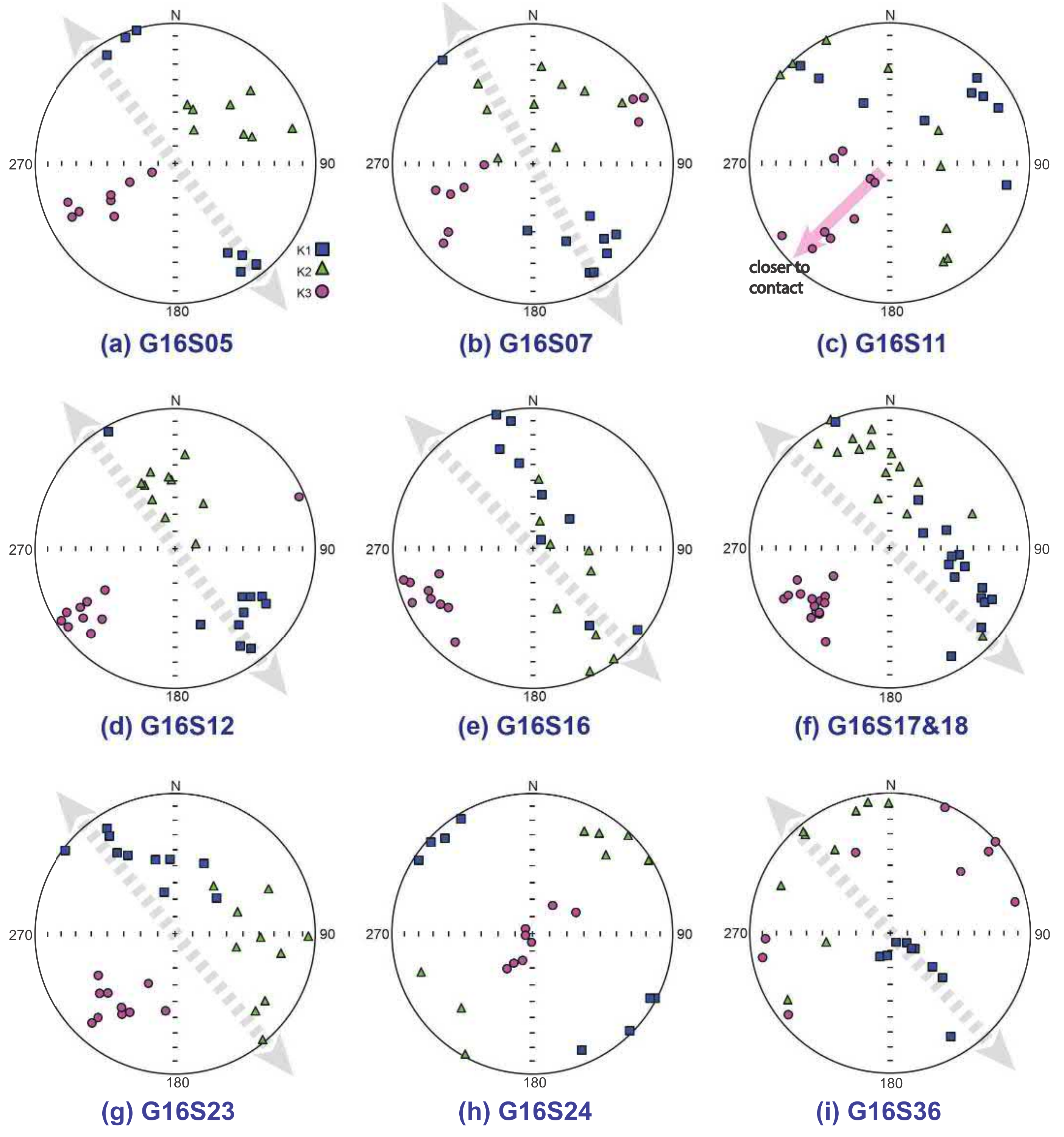


(a) G16S05 (b) G16S07 (c) G16S11

(d) G16S12 (e) G16S16 (f) G16S17&18

(g) G16S23 (h) G16S24 (i) G16S36

# Figure 7

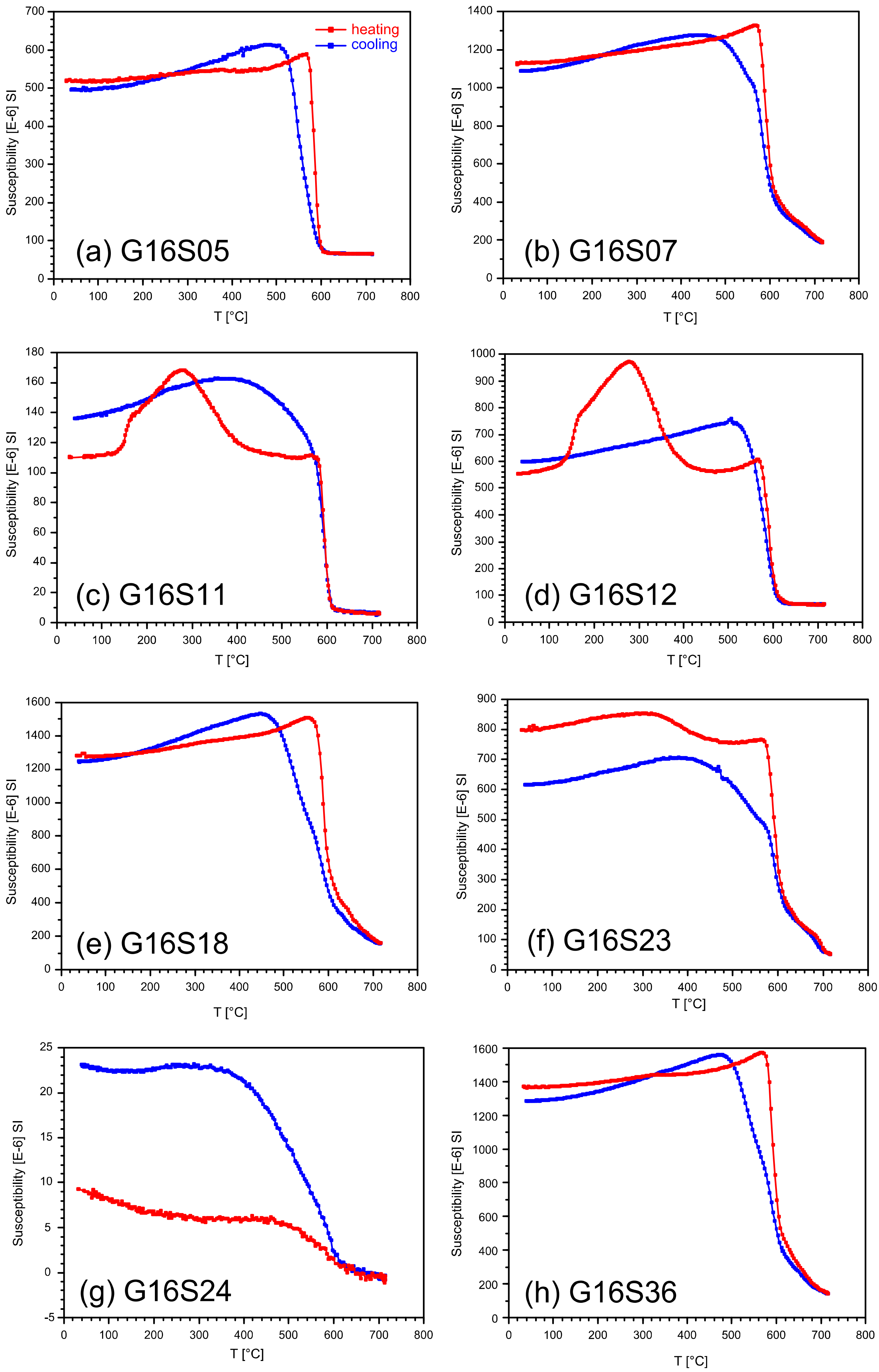

heating
cooling
(a) G16S05
(b) G16S07
(c) G16S11
(d) G16S12
(e) G16S18
(f) G16S23
(g) G16S24
(h) G16S36
Susceptibility [E-6] SI
T [°C]

# Figure 8

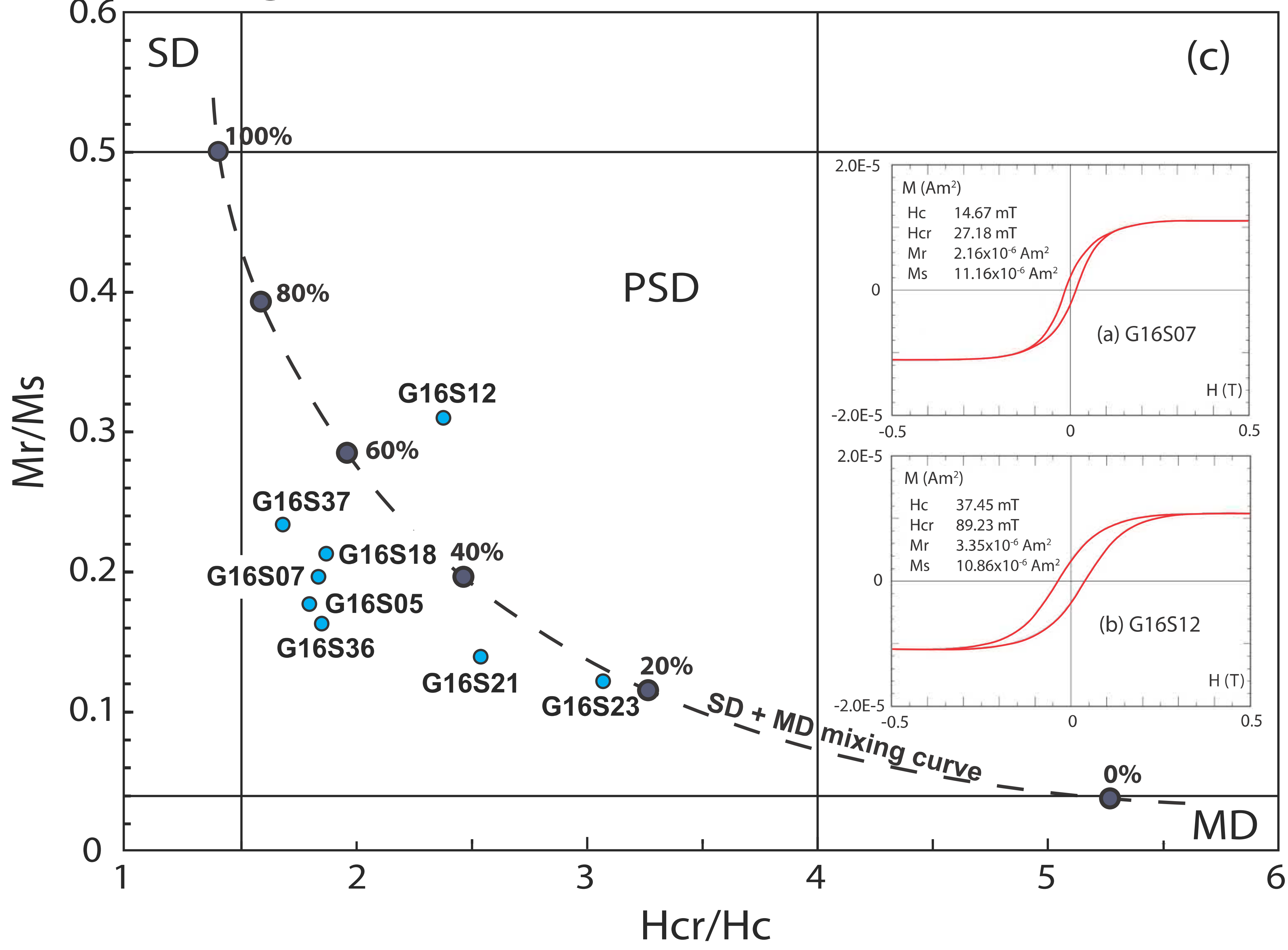

(c)
SD
PSD
MD
Mr/Ms
Hcr/Hc
100%
80%
60%
40%
20%
0%
SD + MD mixing curve
G16S12
G16S37
G16S18
G16S07
G16S05
G16S36
G16S21
G16S23
M (Am²)
Hc 14.67 mT
Hcr 27.18 mT
Mr 2.16x10⁻⁶ Am²
Ms 11.16x10⁻⁶ Am²
(a) G16S07
H (T)
M (Am²)
Hc 37.45 mT
Hcr 89.23 mT
Mr 3.35x10⁻⁶ Am²
Ms 10.86x10⁻⁶ Am²
(b) G16S12
H (T)

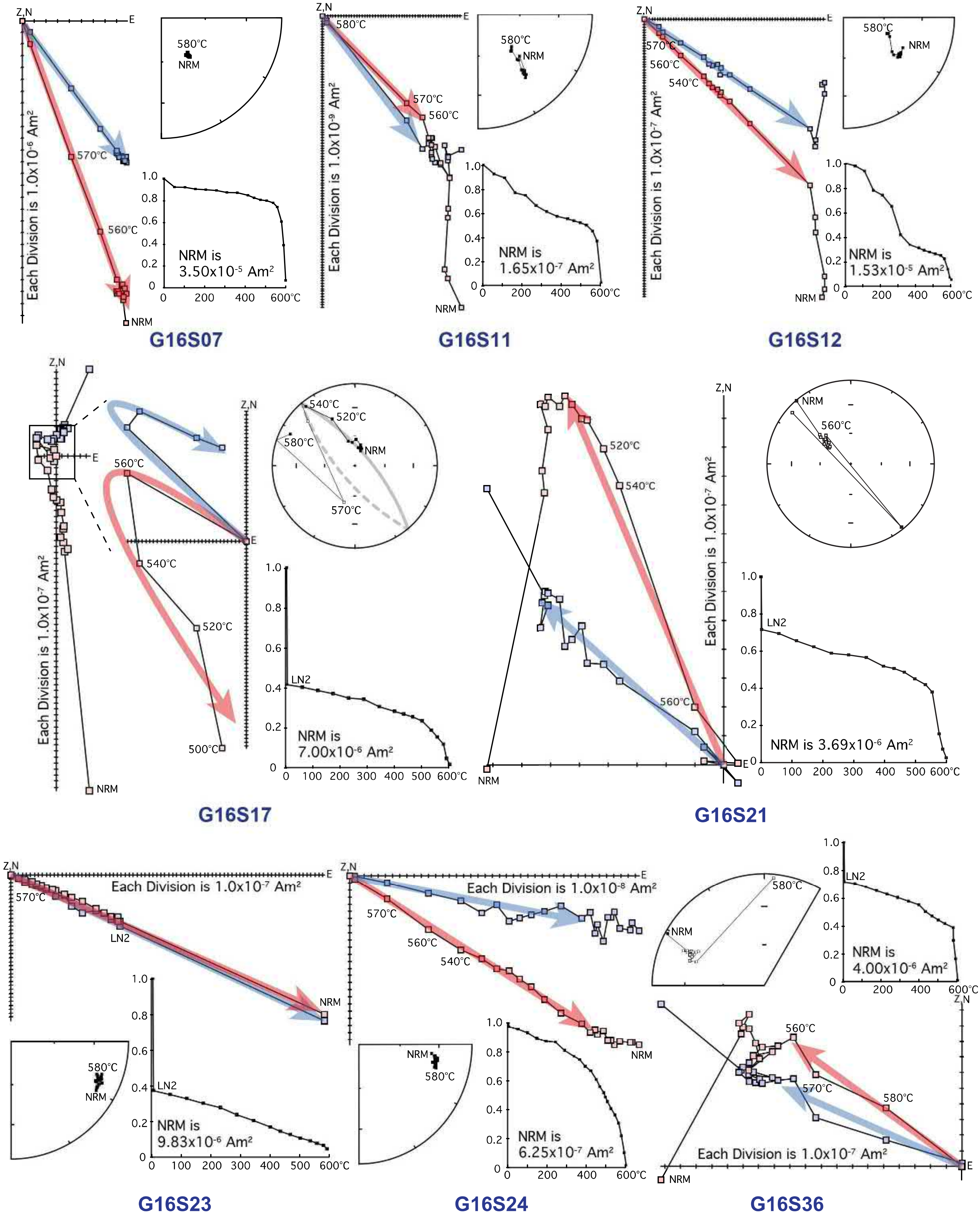
Z,N
E
Each Division is 1.0x10⁻⁶ Am²
580°C
NRM
570°C
560°C
NRM is 3.50x10⁻⁵ Am²
G16S07
Each Division is 1.0x10⁻⁹ Am²
580°C
570°C
560°C
NRM is 1.65x10⁻⁷ Am²
G16S11
Each Division is 1.0x10⁻⁷ Am²
580°C
570°C
560°C
540°C
NRM is 1.53x10⁻⁵ Am²
G16S12
Each Division is 1.0x10⁻⁷ Am²
560°C
540°C
520°C
500°C
580°C
570°C
LN2
NRM is 7.00x10⁻⁶ Am²
G16S17
Each Division is 1.0x10⁻⁷ Am²
520°C
540°C
560°C
LN2
NRM is 3.69x10⁻⁶ Am²
G16S21
Each Division is 1.0x10⁻⁷ Am²
570°C
LN2
580°C
NRM is 9.83x10⁻⁶ Am²
G16S23
Each Division is 1.0x10⁻⁸ Am²
570°C
560°C
540°C
580°C
NRM is 6.25x10⁻⁷ Am²
G16S24
580°C
LN2
NRM is 4.00x10⁻⁶ Am²
560°C
570°C
Each Division is 1.0x10⁻⁷ Am²
G16S36

**Figure 9**

# Figure 10

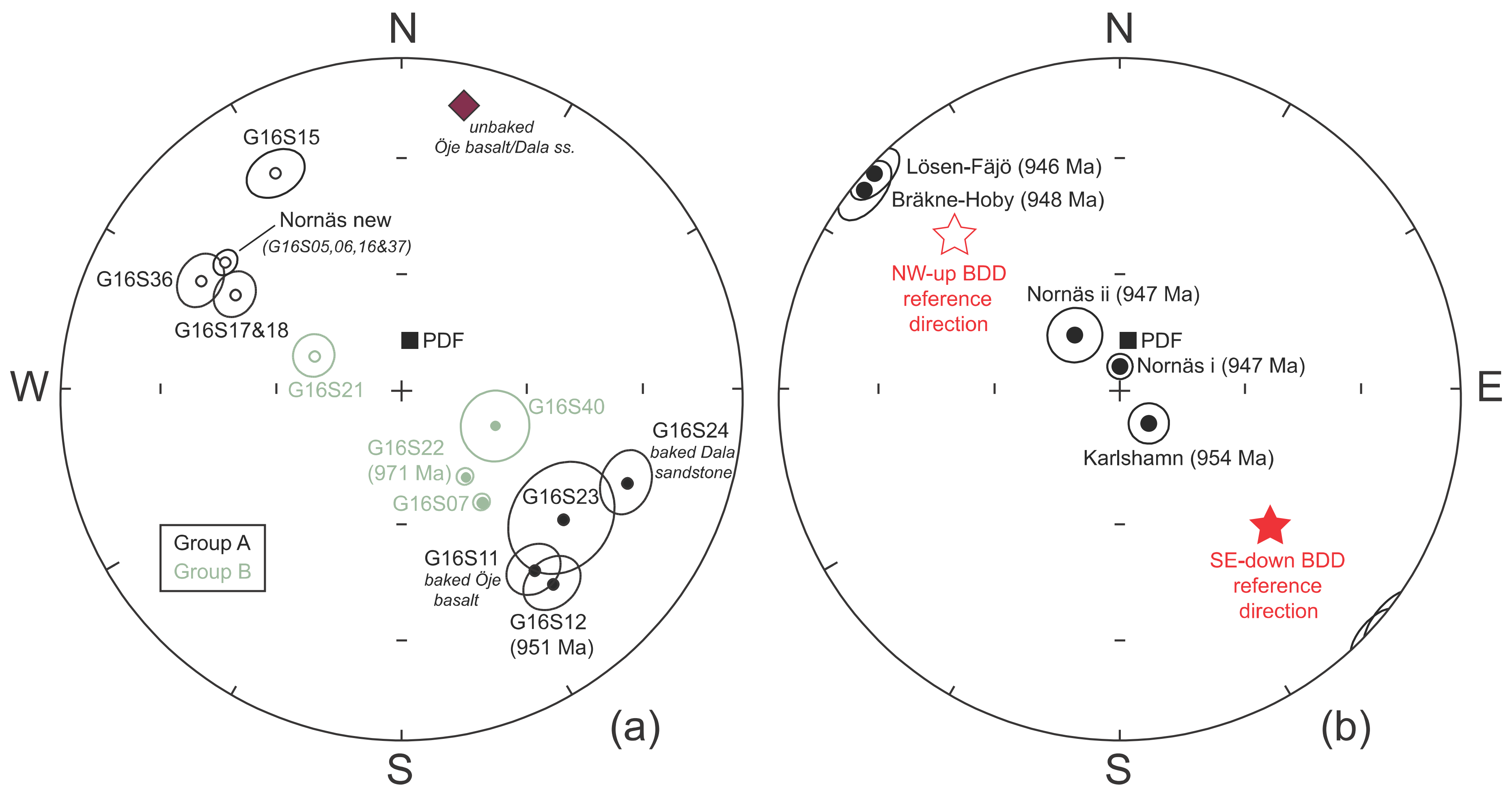
N
W
S
G16S15
unbaked
Öje basalt/Dala ss.
Nornäs new
(G16S05,06,16&37)
G16S36
G16S17&18
PDF
G16S21
G16S40
G16S22
(971 Ma)
G16S07
G16S24
baked Dala
sandstone
G16S23
G16S11
baked Öje
basalt
G16S12
(951 Ma)
Group A
Group B
(a)
N
E
S
Lösen-Fäjö (946 Ma)
Bräkne-Hoby (948 Ma)
NW-up BDD
reference
direction
Nornäs ii (947 Ma)
PDF
Nornäs i (947 Ma)
Karlshamn (954 Ma)
SE-down BDD
reference
direction
(b)

# Figure 11

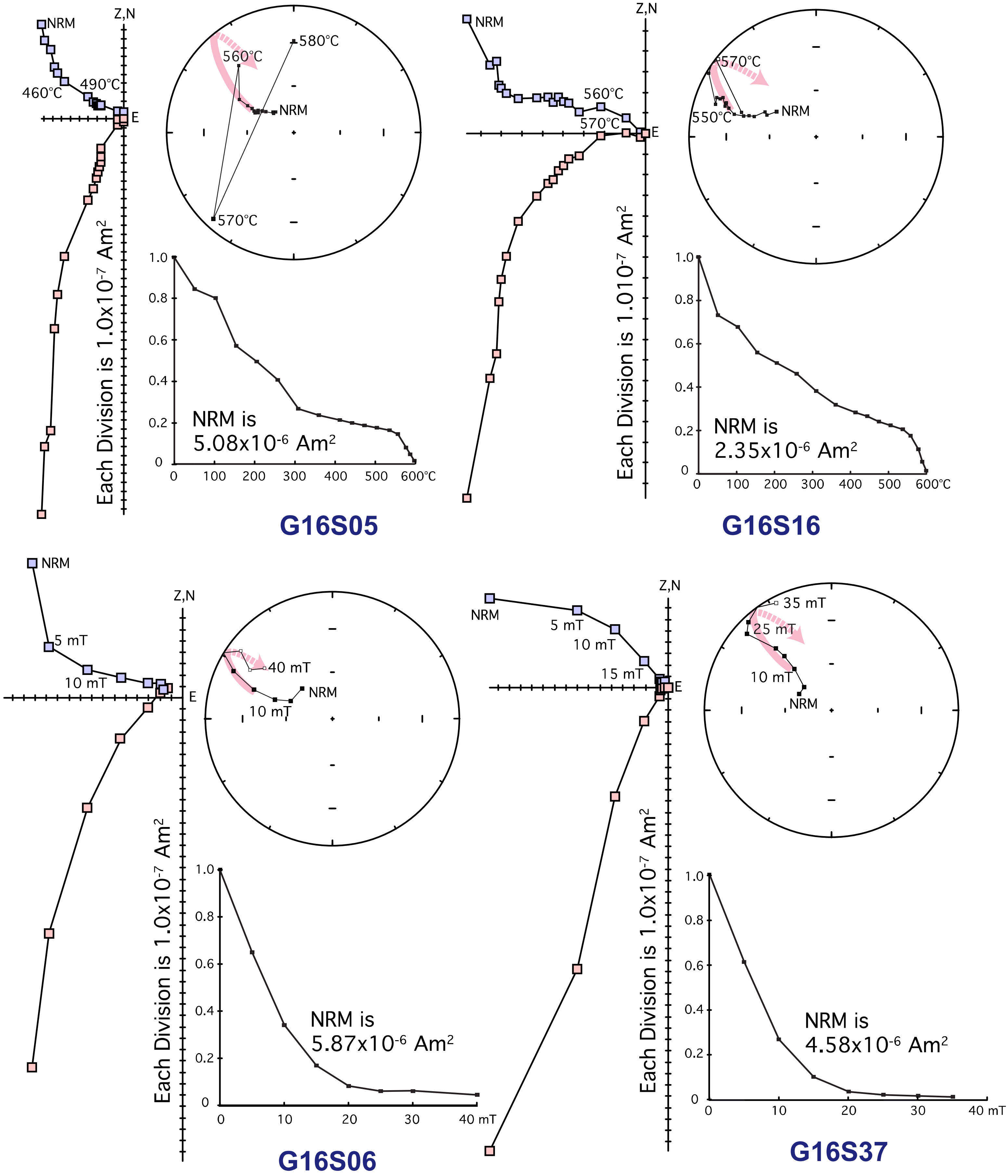
NRM
Z,N
460°C
490°C
E
580°C
560°C
NRM
570°C
Each Division is 1.0x10$^{-7}$ Am$^2$
1.0
0.8
0.6
0.4
0.2
0
0 100 200 300 400 500 600°C
NRM is 5.08x10$^{-6}$ Am$^2$
G16S05
NRM
Z,N
560°C
570°C
E
570°C
550°C
NRM
Each Division is 1.010$^{-7}$ Am$^2$
NRM is 2.35x10$^{-6}$ Am$^2$
G16S16
NRM
5 mT
10 mT
Z,N
E
40 mT
NRM
10 mT
Each Division is 1.0x10$^{-7}$ Am$^2$
0 10 20 30 40 mT
NRM is 5.87x10$^{-6}$ Am$^2$
G16S06
NRM
5 mT
10 mT
15 mT
Z,N
E
35 mT
25 mT
10 mT
NRM
Each Division is 1.0x10$^{-7}$ Am$^2$
NRM is 4.58x10$^{-6}$ Am$^2$
G16S37

# Figure 12

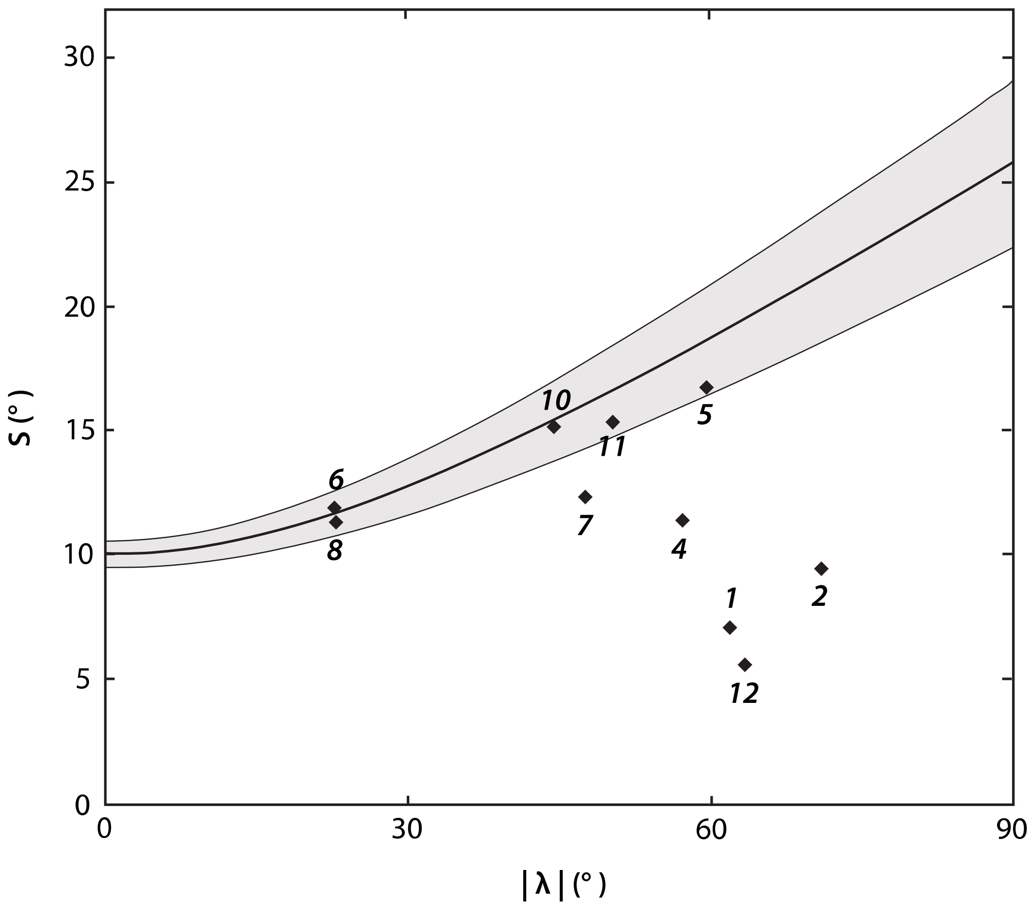

# Figure 13

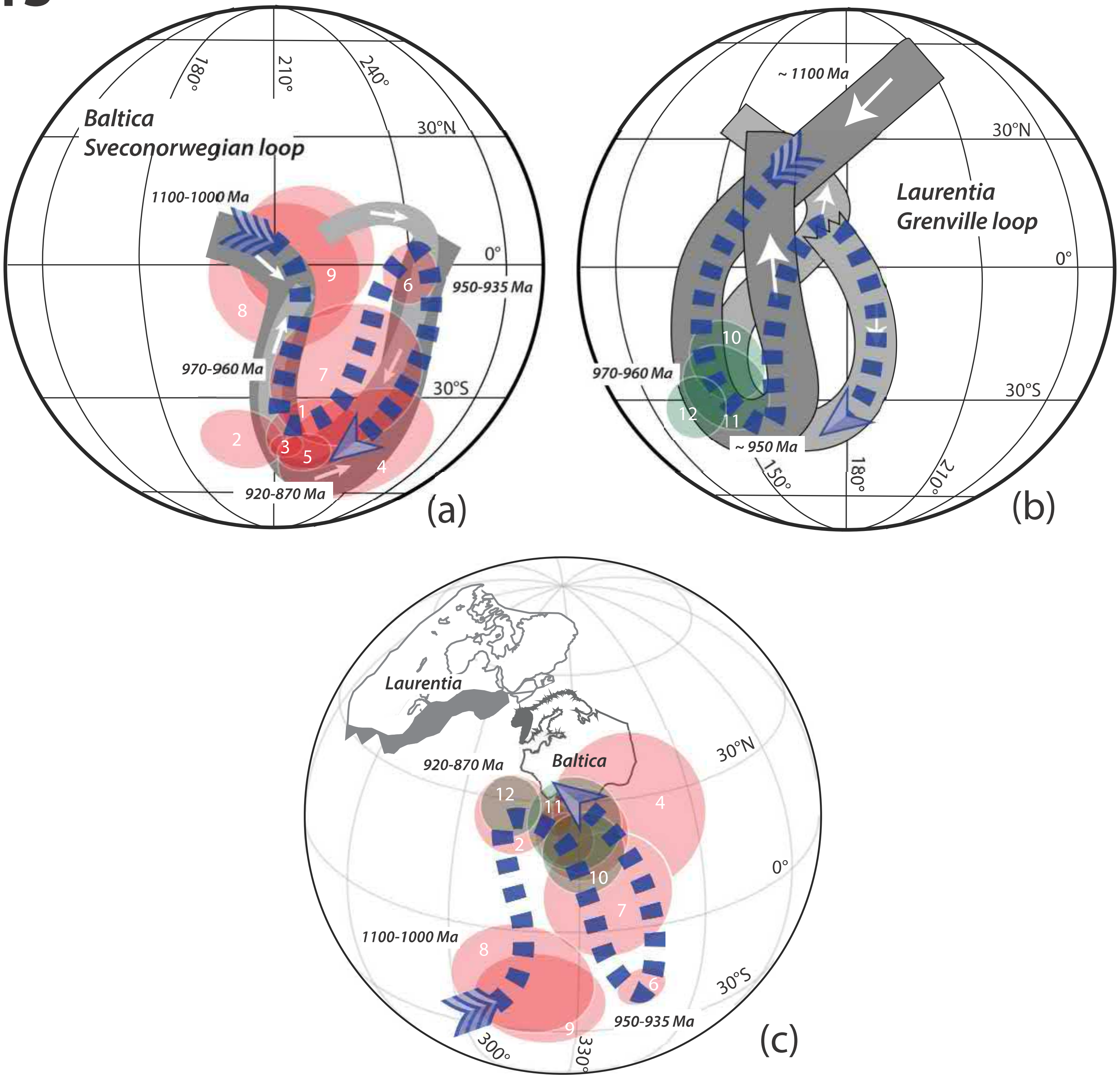
180°
210°
240°
30°N
0°
30°S
Baltica
Sveconorwegian loop
1100-1000 Ma
970-960 Ma
950-935 Ma
920-870 Ma
1
2
3
4
5
6
7
8
9
(a)
~ 1100 Ma
30°N
0°
30°S
150°
180°
210°
Laurentia
Grenville loop
970-960 Ma
~ 950 Ma
10
11
12
(b)
Laurentia
Baltica
920-870 Ma
1100-1000 Ma
950-935 Ma
30°N
0°
30°S
300°
330°
2
4
6
7
8
9
10
11
12
(c)

## Figure 14

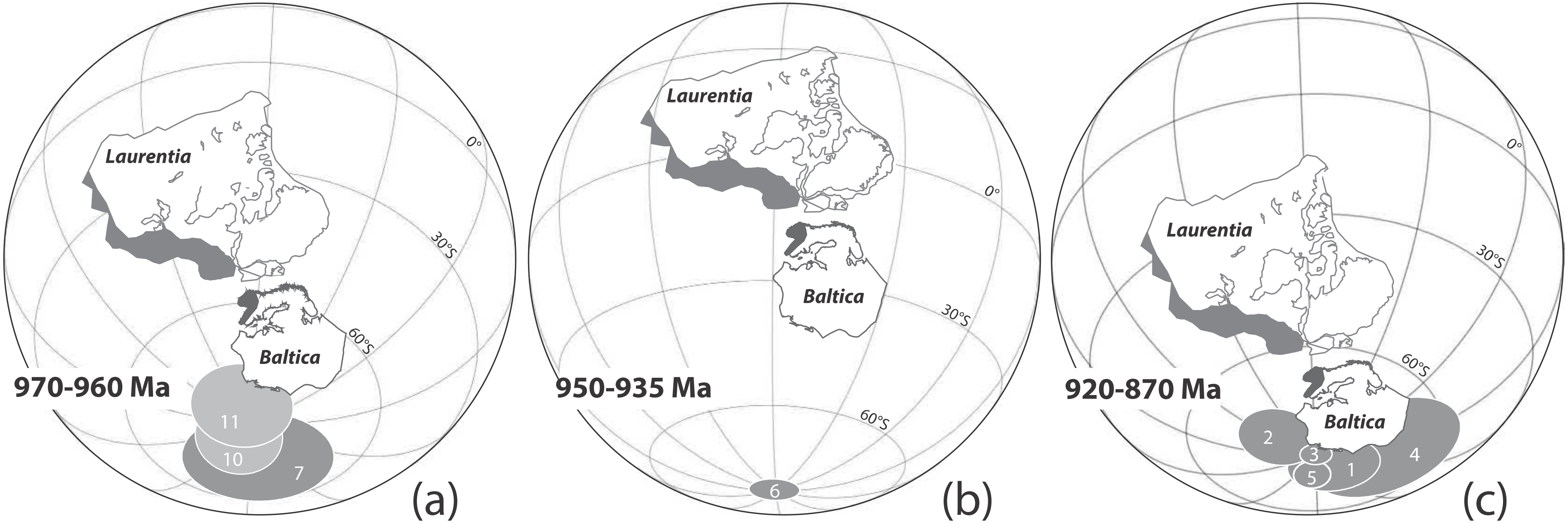

970-960 Ma
Laurentia
Baltica
0°
30°S
60°S
11
10
7
(a)
950-935 Ma
Laurentia
Baltica
0°
30°S
60°S
6
(b)
920-870 Ma
Laurentia
Baltica
0°
30°S
60°S
2
3
5
1
4
(c)

**Table 1 Results of U-Pb baddeleyite geochronology**

| Sample (number of grains) | U/Th | $Pb_c/Pb_{tot}$ [1] | $^{206}Pb/^{204}Pb$ | $^{207}Pb/^{235}U$ | ± 2s% Error | $^{206}Pb/^{238}U$ | ± 2s% Error | $^{207}Pb/^{235}U$ | $^{206}Pb/^{238}U$ | $^{207}Pb/^{206}Pb$ | ± 2σ | Concordance |
|---|---|---|---|---|---|---|---|---|---|---|---|---|
| | | | [Raw][2] | [Corr][3] | | | | [Age, Ma] | | | | |
| *G16S12* | | | | | | | | | | | | |
| Bd-1 (2 grains) | 27.4 | 0.085 | 818.2 | 1.5298 | 1.15 | 0.15711 | 1.10 | 942.4 | 940.7 | 946.5 | 9.2 | 0.994 |
| Bd-2 (4 grains) | 14.3 | 0.046 | 1449.3 | 1.5358 | 0.61 | 0.15707 | 0.51 | 944.8 | 940.4 | 955.1 | 7.0 | 0.985 |
| Bd-3 (3 grains) | 7.3 | 0.174 | 375.2 | 1.5337 | 1.90 | 0.15753 | 1.82 | 944.0 | 943.1 | 946.1 | 15.4 | 0.997 |
| *G16S22* | | | | | | | | | | | | |
| Bd-1 (2 grains) | 5.9 | 0.311 | 214.3 | 1.5922 | 3.96 | 0.16185 | 3.75 | 967.2 | 967.1 | 967.4 | 33.6 | 1.000 |
| Bd-2 (5 grains) | 12.3 | 0.080 | 820.0 | 1.5437 | 0.82 | 0.15688 | 0.73 | 948.0 | 939.4 | 968.0 | 8.4 | 0.970 |
| Bd-3 (5 grains) | 9.0 | 0.168 | 365.5 | 1.5875 | 1.12 | 0.16072 | 0.99 | 965.3 | 960.8 | 975.8 | 11.6 | 0.985 |
| *G16S37* | | | | | | | | | | | | |
| Bd-1 (1 grains) | 13.0 | 0.033 | 2026.6 | 1.5314 | 0.41 | 0.15714 | 0.33 | 943.0 | 940.8 | 948.2 | 5.2 | 0.992 |
| Bd-2 (2 grains) | 17.1 | 0.070 | 947.4 | 1.5281 | 0.74 | 0.15656 | 0.68 | 941.7 | 937.6 | 951.4 | 6.9 | 0.986 |
| Bd-3 (2 grains) | 7.6 | 0.119 | 520.8 | 1.5312 | 0.72 | 0.15773 | 0.65 | 943.0 | 944.1 | 940.3 | 7.0 | 1.004 |

[1] $Pb_c$ = common Pb, $Pb_{tot}$ = total Pb (radiogenic + blank + initial).

[2] Measured ratio, corrected for fractionation and spike.

[3] Isotopic ratios corrected for fractionation (0.1% per amu for Pb), spike contribution, blank (0.4 pg Pb and 0.04 pg U), and initial common Pb. Initial common Pb corrected with isotopic compositions from the model of Stacey and Kramers (1975) at the age of the sample.

**Table 2 Summary of paleomagnetic results of BDD dykes (from North to South)**

| Dyke | Slat (°N) | Slon (°E) | Age (Ma) | Dec (°) | Inc (°) | $\alpha_{95}$ (°) | N/n | Plat (°N) | Plon (°E) | $A_{95}$ (°) | Group | Reference | Comment |
|---|---|---|---|---|---|---|---|---|---|---|---|---|---|
| G16S22 | 61.6043 | 13.2260 | 971 ± 7 | 140.6 | 66.1 | 2.0 | 1/10 | -24.5 | 220.8 | 3.0 | Br | This study | NW-SE trending (324°) |
| G16S21 | 61.5937 | 13.0047 | | 296.5 | -66.5 | 5.0 | 1/8 | -32.1 | 236.3 | 7.5 | Bn | This study | NW-SE trending |
| Nornäs ii | 61.42 | 13.21 | 946.8 ± 1.2 | 325.0 | 71.3 | 6.5 | 1/4 | 71.0 | 282.0 | 10.5 | - | Bylund (1985); Söderlund et al. (2005) | remanance at 10 mT[a] |
| Nornäs i | 61.42 | 13.21 | 946.8 ± 1.2 | 0.4 | 82.2 | 3.0 | 1/6 | 77.0 | 14.0 | 6.0 | - | Piper and Smith (1980); Söderlund et al. (2005) | - |
| G16S05 | 61.4230 | 13.2150 | | Nornäs dyke, partial remagnetization and vector component contamination | | | | | | | - | This study | NW-SE trending (315°) |
| G16S06 | 61.4207 | 13.2202 | | Nornäs dyke, partial remagnetization and vector component contamination | | | | | | | - | This study | NW-SE trending (315°) |
| G16S07 | 61.2557 | 13.7790 | | 142.1 | 58.7 | 2.0 | 1/9 | -15.3 | 223.2 | 2.6 | Br | This study | NW-SE trending (330°) |
| G16S17 | 61.2504 | 13.4103 | | 305.5 | -45.5 | 4.2 | 1/4 | -8.5 | 240.6 | 4.3 | - | This study | NW-SE trending (315°), same dyke as G16S18 |
| G16S18 | 61.2464 | 13.4186 | | 300.5 | -39.8 | 9.4 | 1/5 | -6.4 | 246.6 | 8.7 | - | This study | NW-SE trending (315°), same dyke as G16S17 |
| G16S17&18 comb. | - | - | | 302.2 | -41.7 | 5.2 | 1/9 | -7.0 | 244.6 | 5.0 | An | This study | - |
| G16S24 | 61.1999 | 13.1505 | ~1460 | 110.3 | 30.4 | 6.8 | 1/8 | -5.0 | 257.8 | 5.6 | - | This study | baked Dala sandstone |
| G16S23 | 61.1992 | 13.1515 | | 126.6 | 40.9 | 12.9 | 1/7 | -4.9 | 240.8 | 12.2 | Ar | This study | NW-SE trending (320°) |
| G16S14 | 61.1455 | 12.7273 | | demagnetization behavior like Nornäs dyke, partial remagnetization and vector component contamination | | | | | | | - | This study | NW-SE trending |
| G16S16 | 61.1118 | 13.8530 | | southern extension of Nornäs dyke, partial remagnetization and vector component contamination | | | | | | | - | This study | NW-SE trending (325°), width ~ 8 m |
| G16S15 | 61.0949 | 13.0151 | | 330.7 | -24.7 | 6.2 | 1/3 | 12.4 | 222.1 | 4.7 | An | This study | NW-SE trending (325°) |
| G16S09 | 60.9265 | 13.1784 | | inconsistent directions within dyke | | | | | | | - | This study | NW-SE trending (305°), same dyke as G16S10 |
| G16S37 | 60.9181 | 14.1043 | 947 ± 4 | southern extension of Nornäs dyke, partial remagnetization and vector component contamination | | | | | | | - | This study | NW-SE trending (325°) |
| Nornäs new (G16S05,06,16&37 comb.) | - | - | | 307.9 | -35.3 | 2.9 | 4/22 | -0.8 | 241.7 | 2.6 | - | This study | Mean direction calculated using great circle method |
| G16S10 | 60.8878 | 13.3006 | | inconsistent directions within dyke | | | | | | | - | This study | NW-SE trending (305°), same dyke as G16S09 |
| G16S36 | 60.8284 | 14.2725 | | 300.6 | -32.0 | 5.9 | 1/8 | -1.4 | 249.5 | 5.0 | An | This study | NW-SE trending |
| G16S11 | 60.8077 | 13.5783 | ~1460 | 140.7 | 30.9 | 6.5 | 1/9 | -14.9 | 223.0 | 2.6 | - | This study | baked Öje basalt |
| G16S12 | 60.8077 | 13.5783 | 951 ± 5 | 142.2 | 36.9 | 6.2 | 1/9 | 3.1 | 228.7 | 5.6 | Ar | This study | NW-SE trending (324°) |
| Andersbo | 60.76 | 15.41 | | 143.0 | 42.0 | 9.0 | 1/7 | 1.0 | 229.0 | 7.3 | - | Bylund and Elming (1992) | - |
| G16S13 | 60.7147 | 13.3904 | | 153.2 | 8.3 | 7.3 | 1/8 | 21.8 | 222.4 | 5.2 | - | This study | NW-SE trending |
| Ejen | 60.67 | 14.79 | | 128.0 | 24.0 | 9.0 | 1/8 | 6.0 | 245.8 | 6.6 | - | Bylund (1985) | remanance at 20 mT[a] |
| Falun (new) | 60.59 | 15.58 | 945.7 ± 1.2 | 128.7 | 37.9 | 3.0 | 1/9 | -1.7 | 242.3 | 2.6 | Ar | Elming et al. (2014); Söderlund et al. (2005) | NW-SE trending (330°) |
| Falun (old) | 60.59 | 15.58 | 945.7 ± 1.2 | 131.4 | 45.8 | 5.6 | 1/10 | -6.1 | 237.6 | 5.7 | - | Patchett and Bylund (1977); Söderlund et al. (2005) | remanance at 20 mT[a] |
| Gällsjön | 60.51 | 14.53 | | 136.0 | 48.0 | 12.0 | 1/5 | 18.0 | 241.0 | 8.5 | - | Bylund and Elming (1992) | - |
| G16S40 | 60.3185 | 14.2210 | | 106.0 | 67.0 | 8.3 | 1/9 | -35.0 | 243.7 | 12.5 | Br | This study | NW-SE trending (330°) |
| G16S39 | 60.3024 | 13.8662 | | inconsistent directions within dyke | | | | | | | - | This study | NW-SE trending, same dyke as G16S38 |
| G16S38 | 60.3016 | 13.8672 | | inconsistent directions within dyke | | | | | | | - | This study | NW-SE trending, same dyke as G16S39 |
| Årby | 59.27 | 16.46 | | 142.5 | 52.4 | 7.0 | 1/6 | -7.3 | 227.4 | 8.0 | - | Patchett and Bylund (1977) | remanance at 20 mT[a] |
| Marbystrand | 58.61 | 16.48 | | 127.5 | 31.1 | 3.6 | 1/9 | 3.3 | 246.0 | 3.0 | - | Elming et al. (2014) | NW-SE trending (310°) |
| Y1 | 58.58 | 16.33 | 938 ± 4 | 311.2 | -43.3 | 5.7 | 1/13 | -3.4 | 239.0 | 4.0 | An | Elming et al. (2014) | NE-SE trending (40°) |
| Y2 | 58.58 | 16.33 | 941 ± 6 | 313.3 | -40.7 | 7.4 | 1/14 | -0.5 | 238.3 | 7.0 | An | Elming et al. (2014) | NE-SE trending (40°) |
| Slussen | 58.2 | 12.2 | | 300.9 | -26.5 | 11.5 | 1/6 | 3.2 | 248.5 | 9.2 | An | Pisarevsky and Bylund (2006) | - |
| Tuve | 57.8 | 11.8 | 935 ± 3 | 122.2 | 53.7 | 3.2 | 2/23 | -14.0 | 237.9 | 3.7 | Ar | Pisarevsky and Bylund (2006); Hellström et al. (2004) | - |
| Small | 57.8 | 11.8 | | 124.5 | 54.6 | 7.4 | 1/3 | -13.9 | 235.8 | 8.8 | Ar | Pisarevsky and Bylund (2006) | - |
| Hjuvik | 57.7 | 11.7 | | 118.8 | 37.1 | 11.5 | 1/12 | -3.3 | 246.9 | 10.3 | Ar | Pisarevsky and Bylund (2006) | - |
| Sjunnaryd (sill) | 57.7 | 14.8 | | 317.1 | -28.9 | 15.1 | 1/4 | 8.8 | 236.4 | 12.4 | - | Pesonen and Klein (2014) | - |
| Nilstorp (sill) | 57.64 | 14.83 | 966 ± 5 | 315.2 | -27.4 | 9.7 | 1/6 | 9.0 | 238.5 | 7.8 | - | Patchett and Bylund (1977); Söderlund et al. (2005) | remanance at 40 mT[a] |
| Tärnö | 56.27 | 15.06 | | 312.8 | -41.9 | 4.8 | 1/5 | 0.3 | 237.0 | 4.6 | - | Patchett and Bylund (1977) | remanance at 30 mT[a] |
| Bräkne-Hoby | 56.26 | 15.18 | 948.1 ± 1.4 | 309.3 | 3.6 | 6.1 | 1/7 | 22.2 | 251.9 | 4.3 | - | Patchett and Bylund (1977); Söderlund et al. (2005) | remanance at 40 mT[a] |
| Lösen-Fäjö | 56.17 | 15.69 | 945.8 ± 1.0 | 312.6 | 2.6 | 5.4 | 1/6 | 23.3 | 248.9 | 3.8 | - | Patchett and Bylund (1977); Söderlund et al. (2005) | remanance at 20 mT[a] |
| Väby | 56.17 | 15.22 | | 137.0 | 33.0 | 10.0 | 1/3 | 8.0 | 236.0 | 8.4 | - | Poorter (1975) | remanance at 10 mT[a] |
| Karlshamn | 56.15 | 14.86 | 954.2 ± 1.1 | 129.0 | 81.0 | 4.8 | 1/9 | -43.2 | 213.5 | 9.1 | - | Patchett and Bylund (1977); Söderlund et al. (2004a) | remanance at 30 mT[a] |
| **Group A Mean** | **-** | **-** | | **127.6** | **65.4** | **9.7** | **12/116** | **-2.6** | **239.6** | **5.8** | **-** | | **Averaging 12 dykes in Group An/Ar listed in this table** |
| **Group B Mean** | **-** | **-** | | **128.8** | **39.6** | **6.5** | **4/36** | **-27.0** | **230.4** | **14.9** | **-** | | **Averaging 4 dykes in Group Bn/Br listed in this table** |

Note: Slat/Slon = site geographic latitide/longitude, Dec = declination, Inc = inclination, Plat/Plon = paleomagnetic pole latitude/longitude, N/n = number of site/sample, $\alpha_{95}$ = radius of 95% confidence cone of the mean direction, $A_{95}$ = radius of 95% confidence cone of the paleomagnetic pole

[a] least scatter of data at alternating-field step used for mean vector calculation

**Table 3 Paleomagnetic poles used to constrain the paleogeographic reconstruction of Baltica and Laurentia at ca. 1000-850 Ma**

| # | Paleomagnetic Pole | Dec (°) | Inc (°) | $\alpha_{95}$ (°) | k | N/n | Plat (°N) | Plon (°E) | $A_{95}$ (°) | S (°) | \|λ\| (°) | Age (Ma) | 1 | 2 | 3 | 4 | 5 | 6 | 7 | Q | Reference |
|---|---|---|---|---|---|---|---|---|---|---|---|---|---|---|---|---|---|---|---|---|---|
| ***Baltica*** | | | | | | | | | | | | | | | | | | | | | |
| 1 | Hunnedalen dykes | 294.0 | -75.0 | 6.0 | 115 | 6/69 | -41.0 | 222.0 | 10.5 | 7.2 | 61.8 | 848 ± 27[a]; 855 ± 59[b] | 1 | 1 | 1 | 0 | 1 | 0 | 1 | 5 | Walderhaug et al. (1999) |
| 2 | Egersund-Ogna anorthosite | 325.9 | -80.1 | 4.9 | 73 | 13/69 | -42.1 | 200.4 | 9.0 | 9.5 | 70.8 | 900[c] | 1 | 1 | 1 | 0 | 0 | 0 | 1 | 4 | Brown and McEnroe (2004) |
| 3 | Egersund anorthosite | - | - | - | - | 76/- | -43.5 | 213.7 | 3.6 | - | - | 900[c] | 0 | 1 | 1 | 0 | 0 | 0 | 1 | 3 | Stearn and Piper (1984); Walderhaug et al. (1999) |
| 4 | Rogaland Igneous Complex | 269.0 | -72.0 | 11.0 | 49 | 5/24 | -45.9 | 238.4 | 18.2 | 11.5 | 57.0 | 869 ± 14[a] | 1 | 0 | 1 | 1 | 0 | 0 | 1 | 4 | Walderhaug et al. (2007) |
| 5 | Bjerkreim-Sokndal intrusion | 303.4 | -73.5 | 3.7 | 24 | 66/354 | -35.9 | 217.9 | 6.0 | 16.8 | 59.4 | 916[c] | 1 | 1 | 1 | 0 | 1 | 0 | 1 | 5 | Brown and McEnroe (2015) |
| 6 | Mean 951-935 Ma Baltica pole | 308.8 | -39.6 | 6.5 | 42 | 12/116 | -2.6 | 239.6 | 5.8 | 12.0 | 22.5 | 951-935[d] | 1 | 1 | 1 | 1 | 1 | 1 | 1 | 7 | This study |
| 7 | 971 Ma BDD dykes VGP | 307.6 | -65.4 | 14.2 | 68 | 4/36 | -27.0 | 230.4 | 14.9 | 12.4 | 47.5 | 971 ± 7[d] | 1 | 0 | 1 | 0 | 1 | 1 | 1 | 5 | This study |
| 8 | Laanila-Ristijärvi dykes | 355.5 | -40.0 | 17.5 | 51 | 3/7 | -2.1 | 212.2 | 16.4 | 11.4 | 22.8 | 1042 ± 50[b] | 0 | 0 | 1 | 1 | 1 | 0 | 0 | 3 | Mertanen et al. (1996) |
| 9 | Bamble Intrusion mean | - | - | - | - | - | 3.0 | 217.0 | 15.0 | - | - | 1100-1040 | 0 | 1 | 1 | 0 | 0 | 0 | 0 | 2 | Meert and Torsvik (2003) |
| ***Laurentia*** | | | | | | | | | | | | | | | | | | | | | |
| 10 | Adirondack microcline gneisses | 289.2 | -62.8 | 7.6 | 29 | 14/80 | -18.4 | 151.1 | 10.5 | 15.2 | 44.2 | 960[c] | 1 | 1 | 1 | 0 | 0 | 1 | 1 | 5 | Brown and McEnroe (2012) |
| 11 | Adirondack metamorphic anorthosites and other rocks | 283.9 | -67.3 | 7.7 | 28 | 14/68 | -25.1 | 149.0 | 11.6 | 15.4 | 50.1 | 970[c] | 1 | 1 | 1 | 0 | 0 | 1 | 1 | 5 | Brown and McEnroe (2012) |
| 12 | Adirondack fayalite granites | 297.0 | -75.8 | 3.9 | 199 | 8/40 | -28.4 | 132.7 | 6.9 | 5.7 | 63.2 | 990[c] | 1 | 1 | 1 | 0 | 0 | 1 | 1 | 5 | Brown and McEnroe (2012) |

Note: Dec = declination, Inc = inclination, $\alpha_{95}$ = radius of 95% confidence cone of the mean direction, k = precision parameter, N/n = number of site/sample, Plat/Plon = paleomagnetic pole latitude/longitude, $A_{95}$ = radius of 95% confidence cone of the paleomagnetic pole, S = angular dispersion of VGPs, |λ| = absolute value of paleolatitude, Q = sum of quality criteria (Van der Voo, 1990)

[a] Ar-Ar biotite ages

[b] Sm-Nd whole rock ages

[c] Cooling ages

[d] U-Pb baddeleyite ages